3-27-2015 12:00 AM

Three-Dimensional Computed Tomography Measurements of Pulmonary Artery Volumes: Development and Application

Tamas J. Lindenmaier
The University of Western Ontario

Supervisor
Dr. Grace Parraga
The University of Western Ontario

Graduate Program in Medical Biophysics
A thesis submitted in partial fulfillment of the requirements for the degree in Master of Science
© Tamas J. Lindenmaier 2015

THREE-DIMENSIONAL COMPUTED TOMOGRAPHY MEASUREMENTS OF PULMONARY ARTERY VOLUMES: DEVELOPMENT AND APPLICATION

(Thesis format: Integrated Article)

by

Tamas J. <u>Lindenmaier</u>

Graduate Program in Medical Biophysics

A thesis submitted in partial fulfillment
of the requirements for the degree of
Master of Science

The School of Graduate and Postdoctoral Studies
The University of Western Ontario
London, Ontario, Canada

Abstract

Chronic obstructive pulmonary disease (COPD) is a major contributor to hospitalizations and healthcare costs in North America. While the hallmark of COPD is airflow limitation, it is also associated with abnormalities of the cardiovascular system. Enlargement of the pulmonary artery (PA) is a morphological marker of pulmonary hypertension, and was previously shown to predict acute exacerbations using a one-dimensional (1D) diameter measurement of the main PA. We hypothesized that a three-dimensional (3D) quantification of PA size would be more sensitive than 1D methods and encompass morphological changes along the entire central PA. Hence, we developed a 3D measurement of the main (MPA), left (LPA) and right (RPA) pulmonary arteries as well as total PA volume (TPA) volume from thoracic x-ray computed tomography (CT) imaging. Three observers performed five repeated measurements for 15 ex-smokers. There was a strong agreement ($r^2 = 0.76$) between PA volume and PA diameter measurements, which was used as the gold standard. Intra-rater measurement reproducibility was evaluated by calculating the coefficient of variation (CV) using five rounds of measurements and revealed excellent agreement (CV < 8%) between measurements. Inter-rater measurement variability was also evaluated using intraclass correlation analysis which revealed strong agreement ($ICC_{MPA}=0.98$) between observers.

In an application of this tool, we sought to explore the relationship between PA volumes and lung structure-function as determined by spirometry, hyperpolarized helium-3 magnetic resonance imaging (MRI) and CT in 124 ex-smokers, with (n=68) and without (n=56) airflow limitation, and in a control group of 35 healthy never-smokers. We observed significantly greater MPA (p=.014), RPA (p=.001) and TPA (p=.003) volumes in ex-smokers with airflow limitation when compared to ex-smokers without airflow limitation. We also observed significantly greater PA volumes in both ex-smoker subgroups when compared with the never-smoker control group. Modest but significant correlations were observed for PA volumes and measurements of lung structure and function. However, this was not observed when analyzing ex-smokers with airflow limitation alone, suggesting that pulmonary artery enlargement may occur secondary to

COPD in our subject group. Multivariate zero-inflated Poisson regression analysis revealed TPA volume to be a significant (p=.03) predictor of acute exacerbations of COPD.

In conclusion, we developed a reproducible technique for quantifying the volume of the PA. We showed that pulmonary artery enlargement may be secondary to COPD in our subject group. We also showed that total pulmonary artery volume was a significant predictor of COPD exacerbations and could be considered as a biomarker for predicting the occurrence of exacerbation events. Automated measurements of pulmonary artery abnormalities once developed, can be used to further evaluate healthy volunteers and patients with COPD.

Co-Authorship Statement

The following thesis contains manuscripts that have been submitted for publication or are in preparation to be submitted to peer-reviewed scientific journals. Chapter 2 encompasses the original manuscript entitled "Three-Dimensional Segmentation of Pulmonary Artery Volume from Thoracic Computed Tomography Imaging" submitted to *SPIE Medical Imaging, Conference Proceedings* (January 14, 2015), authored by Tamas J. Lindenmaier, Khadija Sheikh, Emma Bluemke, Igor Gyacskov, Marco Mura, Christopher Licskai, Lisa Mielniczuk, Aaron Fenster, Ian A. Cunningham and Grace Parraga. Chapter 3 encompasses the original manuscript entitled "Pulmonary Artery Abnormalities in Ex-smokers with and without Airflow Limitation" to be submitted to the *Journal of COPD* (April, 2015), authored by Tamas J. Lindenmaier, Miranda Kirby, Gregory Paulin, Marko Mura, Christopher Licskai, Harvey O. Coxson, Ian A. Cunningham and Grace Parraga. As principal author and Master's candidate, Tamas J. Lindenmaier developed a three-dimensional technique for evaluating the size of the pulmonary artery using previously developed software originally intended for carotid artery analyses. Tamas J. Lindenmaier performed all main, left, right and total pulmonary artery measurements, pulmonary artery diameter measurements, as well as aorta diameter measurements. Tamas J. Lindenmaier also constructed the main database, performed data analyses, and composed the original drafts of the manuscripts. Miranda Kirby performed analyses of computed tomography and hyperpolarized helium magnetic resonance images to obtain measurements of lung function and structure. Emma Bluemke and Khadija Sheikh participated in image analysis and served as the second and third observers for determining inter- and intra-observer variability. Igor Gyacskov contributed to the tool development for 3D measurements of PA volumes. Drs. Marco Mura, Christopher Licskai, Lisa Mielniczuk and Ian A. Cunningham formed the advisory committee, provided guidance and support, contributed ideas to the construction of the manuscripts and provided feedback for manuscripts. Drs. Aaron Fenster and Harvey O. Coxson provided feedback for the revision of the manuscripts. Dr. Grace Parraga supervised Tamas J. Lindenmaier, helped determine research objectives and provided guidance, mentorship and editorial assistance. Data analyzed for this thesis were part of the ongoing study by the Thoracic Imaging Network of Canada (TINCan).

Computed tomography imaging was performed at University Hospital, London, Ontario, Canada.

To my loving family and friends
for your guidance throughout this journey.

Acknowledgments

I would like to acknowledge my supervisor Dr. Grace Parraga for providing me with a lifelong experience in her laboratory. When I first joined her lab as an undergraduate student, I knew nearly nothing about what research was. This changed very quickly during my undergraduate training and thesis. I was very pleased with Dr. Parraga's offer to become her graduate student and complete my Master's degree under her supervision. I have learned many things from Dr. Parraga; but most important of all she has thought me how to be productive and how to juggle multiple ongoing tasks at once. Dr. Parraga was always available, quickly returning time-sensitive manuscripts so that the next set of changes could be made. I would like to thank Dr. Parraga for the opportunity she has given me, the ample amount of support she provided and the doors she has opened for my future.

I would like to thank the other members of my advisory committee, Drs. Marco Mura, Christopher Licskai, Ian A. Cunningham and Lisa Mielniczuk, for taking time away from their busy schedules to provide me with guidance and support. Your criticism has been helpful in developing new ideas throughout my project and your comments have made my manuscripts complete.

I would like to thank all my lab mates for their help and moral support through the past few years and for being more than just colleagues. Your friendships mean a lot to me and I will always cherish the great times we had together. Even though some of you graduated before I started my Master's degree, I am thankful for how much I have learned from you. I would have not succeeded without your help and support. Dan, thank you for being patient with me throughout my training days. I will never forget our carotid artery segmentation marathons. Miranda, thank you for being a great role model. Thank you for all you have taught me and for pushing me to try and answer questions on my own. Nikhil, thank you for keeping me company in the dark room through those long segmentation days

Table of Contents

List of Tables

Chapter 1:

Chapter 3:

List of Figures

Chapter 3:

List of Appendices

List of Abbreviations

3D	Three-dimensional
6MWD	Six-minute walk distance
ADC	Apparent diffusion coefficient
ATP	Adenosine triphosphate
BF	Bifurcation
COPD	Chronic obstructive pulmonary disease
CT	Computed tomography
CV	Coefficient of variation
DLCO	Diffusing capacity of carbon monoxide
ERV	Expiratory reserve volume
FEV1	Forced expiratory volume in one second
FRC	Functional residual capacity
FVC	Forced vital capacity
HU	Hounsfield units
IC	Inspiratory capacity
ICC	Intraclass correlation coefficient
IRV	Inspiratory reserve volume
ISD	Inter-slice distance
LPA	Left pulmonary artery
LPAV	Left pulmonary artery volume
mMRC	Modified Medical Research Council
MPA	Main pulmonary artery
MPAV	Main pulmonary artery volume
MRI	Magnetic resonance imaging
PA	Pulmonary artery
PH	Pulmonary hypertension
RPA	Right pulmonary artery
RPAV	Right pulmonary artery volume
RV	Residual volume
SGRQ	St. George's respiratory questionnaire
TLC	Total lung capacity
TPA	Total pulmonary artery
TPAV	Total pulmonary artery volume
TV	Tidal volume
VC	Vital capacity
VDP	Ventilation defect percent
%pred	Percent predicted

CHAPTER 1: INTRODUCTION

Individuals with Chronic Obstructive Pulmonary Disease (COPD) often experience acute exacerbations which are severe events associated with an increase in morbidity and mortality. Previous work[1] demonstrated that abnormalities of the pulmonary artery are predictive of these events; however, further research and better tools are needed to strengthen this finding. The purpose of this chapter is to provide motivation for the work presented in subsequent chapters and to provide an overview of pulmonary anatomy, lung function, pulmonary artery anatomy and current biomarkers used to predict the occurrence of acute exacerbations of COPD.

1.1 Overview

Chronic obstructive pulmonary disease (COPD) is a chronic, obstructive, inflammatory disease affecting millions of individuals. It mainly manifests in elderly individuals who have been exposed to tobacco smoke and air pollution for extended periods of time.[2] These toxins induce an inflammatory response in the lungs, resulting in a combination of small airways disease (obstructive bronchiolitis) and parenchymal destruction (emphysema), the extent of which varies among individuals.[3] Persons with COPD are associated with a decline in lung function and an increase in airflow limitation. As the disease progresses, those with moderate-to-severe disease are likely to experience acute events known as exacerbations, often resulting from bacterial or viral infections.[4] These individuals experience a reduced quality of life and seek immediate medical attention which often results in hospitalization. Costs associated with treatment substantially burden our healthcare system. While COPD is preventable and treatable, it is very rarely reversible. Current diagnosis relies on spirometry measurements as it is the most widely available diagnostic tool that can provide global measurements of the lung.

Although the defining feature of COPD is airflow limitation, COPD is also associated with vascular abnormalities such as coronary vascular disease, cerebrovascular disease[5-8] and pulmonary artery (PA) anomalies.[1] Vascular disease is the leading cause of hospitalization for individuals with mild to moderate cases of COPD and following cancer, it ranks as the second leading cause of death.[9, 10] Those with COPD can often develop mild cases of pulmonary hypertension (PH), while some can progress to develop out of proportion PH, which has also been linked to abnormalities in the PA.[11] While previous studies have

utilized a simple one-dimensional diameter measurement of the main PA (MPA) to quantify its size, a more robust, three-dimensional (3D) measurement for assessing PA volumes has not yet been developed. Thus, our goal was to develop 3D metrics to evaluate the size of the main, left (LPA) and right (RPA) pulmonary arteries and to explore their relationships with measurements of lung function and structure as determined by spirometry, CT and hyperpolarized helium-3 magnetic resonance imaging (MRI) of the lung.

The second chapter of this thesis focuses on the development of the 3D measurement for quantifying MPA, LPA, RPA and total PA (TPA) volumes. Intra- and inter-observer as well as longitudinal reproducibility was assessed and reported. The third chapter focuses on the relationship between MPA, LPA, RPA and TPA volumes with measurements of lung function and structure as well as on the ability of the 3D volumetric technique in predicting future exacerbations of COPD. The fourth and final chapter of this thesis serves as a summary. As well, it focuses on the limitations of the current techniques outlining ideas that might be worth exploring in the future.

1.2 Burden of COPD

As outlined by The Global Burden of Disease set by the World Health Organization, respiratory disease accounted for 6.8 and 6.9 percent of female and male deaths worldwide.[12] Furthermore, COPD has ranked as the fourth leading cause of death worldwide accounting for 3.0 million or 5.1% of all deaths worldwide.[12] In 2012, COPD was ranked as the fourth leading cause of death in lower-middle income countries, next to ischemic heart disease, stroke and lower respiratory infections, causing a total of 3.1 million deaths worldwide.[13] To date, there are 64 million people who suffer from mild-to-moderate cases of COPD and this number is on the rise. Projections for 2030 predict COPD to climb to be the third leading cause of death worldwide, accounting for 8.6% of all deaths, a 3.5% increase from 2004 in total deaths due to COPD.[14] The leading causes of death for 2004 and projections for 2030 are summarized in Table 1-1. Interestingly, vascular disease is the single largest cause of hospitalization for individuals with mild-to-moderate cases of COPD, and following lung cancer, the second leading cause of death.[9, 10] In a recent study[9] of 5887 middle-aged volunteers with asymptomatic airway obstruction who quit smoking

at the baseline visit, 22% of subject deaths were caused by cardiovascular disease, second to 33% of lung cancer deaths, 14.5 years into the study.[9] Thus, it is important to consider and explore in detail the relationship between COPD and cardiovascular disease to better understand the mechanisms responsible for such outcomes.

Table 1-1 Leading causes of death as determined by the WHO.[14]

Disease or Injury	2004		2030	
	Deaths (%)	Rank	Rank	Deaths (%)
Ischemic heart disease	12.2	1	1	14.2
Cerebrovascular disease	9.7	2	2	12.1
Lower respiratory infections	7.0	3	4	3.8
COPD	5.1	**4**	**3**	8.6

1.3 Lung Structure and Function

Human cells require oxygen from the surrounding environment to produce energy in the form of adenosine triphosphate (ATP) through a process called cellular respiration. A byproduct of this process is carbon dioxide, which must be removed and released back into the environment.[15] The primary function of the lungs is gas exchange, delivering oxygen from the environment into our circulating blood as well as removing carbon dioxide and releasing it back into the environment.[16] Figure 1-1 outlines the human airway tree, the path inhaled air takes to reach the alveolar sacs (alveoli) of the lungs, where the majority of gas exchange occurs. The airways are made up of branching tubes which become progressively narrower and shorter and increase in number towards the alveolar sacs.[16] Airways can be divided into two major categories, those in the conducting zone and those in the respiratory zone. Conducting airways are responsible for transporting air to smaller airways where gas exchange can take place. Conducting airways are not responsible for gas exchange as they do not contain alveoli.[16] Respiratory airways however contain alveoli and therefore are responsible for gas exchange. Most of the gas exchange occurs in the alveoli which are the most distal part of the airway tree.[16] The following subchapters will outline the roles of the conducting and respiratory airways in more detail.

1.3.1 Conducting zone

The conducting zone is comprised of the upper and lower airways. The upper airways include the nose, oral cavity, pharynx and the larynx.[17] They are responsible for being the

primary conductors of air, for warming and humidifying the inspired air and for preventing foreign materials from entering the airways.[17] Following the upper airways, inhaled air travels through the lower airways (conducting airways) which in general include the first 16 generations (orders) of the tracheobronchial tree.[16, 17] As shown in Figure 1-1, the airway tree starts off at generation zero, or the trachea, which then divides into the left and right main bronchi which enter the left and right lung respectively.[16] The airway tree continues dividing in a dichotomous fashion, meaning that every mother branch bifurcates into two daughter branches, that can be different in size, first into bronchioles and then the terminal bronchioles.[15, 16, 18] The terminal bronchioles are generally the 16th generation airways and are the final airways that make up the conducting zone. Besides directing air to the respiratory zone, the conducting airways further warm and humidify the inhaled air to make it more efficient for gas exchange. The walls of these airways are generally composed of three different layers. The inner epithelial layer is lined with epithelial cells that are equipped with cilia and numerous mucus glands. These form the mucociliary escalator and work together to expel foreign particles.[15, 17] Trapped particles in the mucus travel upstream at a rate of about 2 mm/s to the pharynx, where the mucus is swallowed.[15] The middle layer of the wall is a smooth muscle layer while the outermost layer is composed of connective tissue containing supportive cartilage.[15] Both layers provide the conductive airways' rigidity and support. Due to the lack of alveoli, the conductive airways do not play a role in gas exchange. Thus, they constitute the anatomic dead space which is about 150 mL in volume.[16]

1.3.2   Respiratory zone

The respiratory zone is comprised of airway generations 17 to 23. The respiratory bronchioles are the first airways to form alveoli and therefore some of the gas exchange occurs in these airways.[16] As shown in Figure 1-1, downstream from the respiratory bronchioles, the alveolar ducts form more alveoli and thus, more gas exchange can take place in these airways. Generation 23 is usually the last branch of the airway tree and these are the alveolar sacs which are completely lined with alveoli. This is where most of the gas exchange takes place.[16] Gas exchange follows simple diffusion, as described by Fick's law of diffusion, outlined in Equation 1 below, where A is the area of diffusion, D is the

diffusion coefficient of gas, P_1 and P_2 are the partial pressures of the gas on either side of the alveolar membrane and finally, T is the thickness of the membrane.

$$Diffusion = \frac{A \cdot D \cdot (P_1 - P_2)}{T} \qquad (1)$$

		Generation
	Trachea	0
	Bronchi	1
		2
		3
	Bronchioles	4
		5
	Terminal bronchiloes	16
		17
	Respiratory bronchioles	18
		19
		20
	Alveolar ducts	22
	Alveolar sacs	23

Conducting Zone · Respiratory Zone
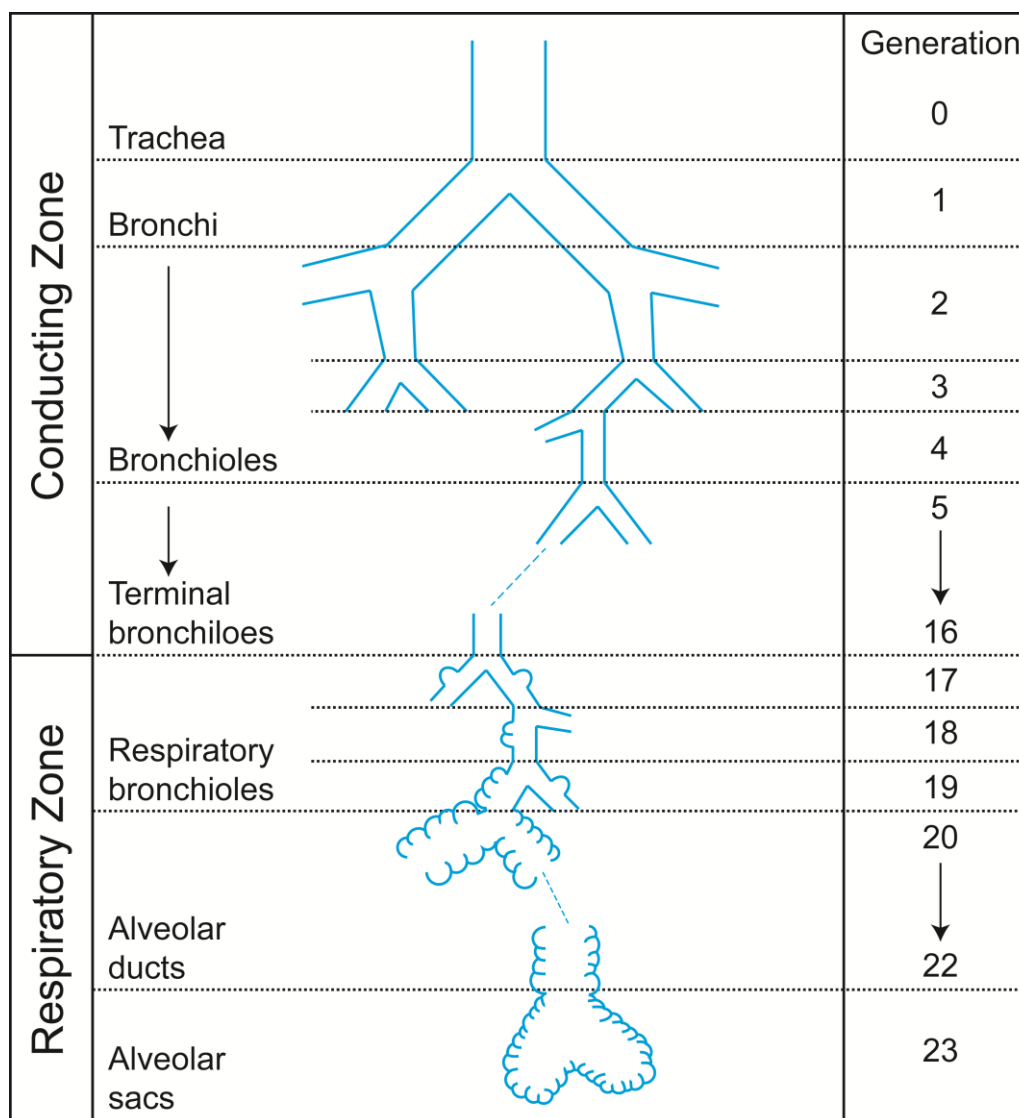
Figure 1-1: Human airway tree. This diagram is not drawn to scale. The first 16 generations represent the conducting zone while generations 17-23 represent the respiratory zone of the airways. Image adapted from West JB, Respiratory Physiology; The Essentials[16]

Diffusion of oxygen across the alveolar membrane occurs from an area with high partial pressure inside the alveoli to low partial pressure in the pulmonary capillaries.[16] Since the

alveolar membrane is very thin and has a large area between 50 and 100 square meters, it is very well suited for efficient diffusion to occur.[16] Since respiratory airways do not have a mucociliary escalator like conductive airways, macrophages remove waste and particles by carrying them either to the mucociliary escalator or into the bloodstream.[15]

1.4 Established methods for measuring lung function

Several techniques have emerged to assess the function of the lung. Pulmonary function tests provide a quantitative evaluation of global lung function and include spirometry, plethysmography and diffusing capacity of carbon monoxide (DL_{CO}).[19] The six-minute walk distance (6MWD)[20] test provides a means of evaluating exercise capacity and breathlessness. Qualitative measures of lung function include the modified Medical Research Council (mMRC) dyspnea scale[21] as well as the St. George's Respiratory Questionnaire (SGRQ).[22, 23] These tests are relatively inexpensive making them widely available and useful tools in the clinical setting as well as in research. In the following sections, I will describe these tests in more detail.

1.4.1 Pulmonary function tests

Pulmonary function tests provide global measurements of the overall function of the lung. Spirometry, which is the most common test and most widely seen in the clinic, measures dynamic flow rates using a spirometer (Figure 1-2A) and is the current gold standard for measuring lung function. During a spirometry test, the subject is first instructed to take a deep breath all the way in and then is asked to blast the air out as hard and as fast as possible, all the way out, through the mouthpiece of the instrument. This maneuver provides us with two parameters, the forced expiratory volume in one second (FEV_1), which is the amount of air that can be forcefully exhaled in the first second of the maneuver, and the forced vital capacity (FVC), which is the total amount of air that can be exhaled from the lungs, as shown in Figure 1-2B. The patient then returns to normal breathing.

A

B
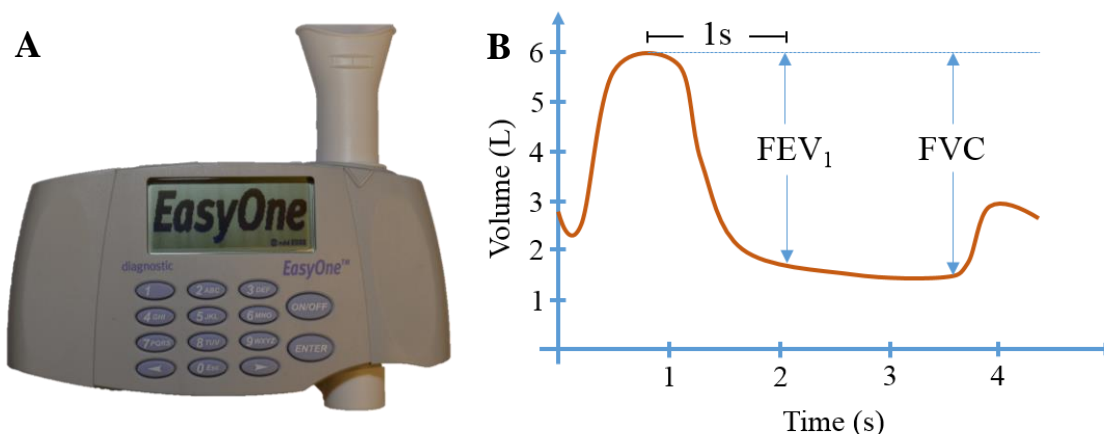
Figure 1-2: Spirometry measurement. Panel A shows an EasyOne hand-held spirometer. To perform a measurement, the subject takes a deep breath all the way in, then is asked to blast the air as fast and hard as possible all the way out through the mouthpiece. Panel B shows the airflow curve for this maneuver with the forced expiratory volume in one second and forced vital capacity overlaid.

A plethysmograph, shown in Figure 1-3A, is an instrument which provides a closed system environment that measures pressure differences and utilizes Boyle's law, to calculate static lung volumes. Boyle's law is shown in Equation 2, where P_l and V_l are the pressure and the volume of gas in the lung respectively, while P_b and V_b are the pressure and volume in the box.

$$P_l V_l = P_b V_b \qquad (2)$$

Volumes that can be obtained using plethysmography are total lung capacity (TLC), the total amount of air that is present in the lungs after maximum inhalation; tidal volume (TV), the amount of air inhaled and exhaled during regular breathing at rest; functional residual capacity (FRC), the amount of air present in the lungs at the end of a normal breath at rest; expiratory reserve volume (ERV), the volume of air that can be exhaled after completing a regular exhalation at rest; residual volume (RV), the amount of air that remains in the lungs after maximal exhalation; inspiratory reserve volume (IRV), the maximum amount of gas that can be inhaled after completing a normal inhalation at rest; vital capacity (VC), the total amount of air that can be exhaled after the deepest inspiration; inspiratory capacity (IC), the total amount of air that can be inhaled after a normal exhalation at rest. To obtain

these volumes, shown in Figure 1-3B, subjects are instructed to start with normal breathing while seated in the closed system. When they reach FRC a shutter closes, blocking the flow of air from entering and exiting the lungs. As the subject attempts to breathe against the shutter, the pressure in the lungs decreases and the volume increases causing the pressure in the box to increase and the volume to decrease. Boyle's law is then used to find the volume of air in the lungs.
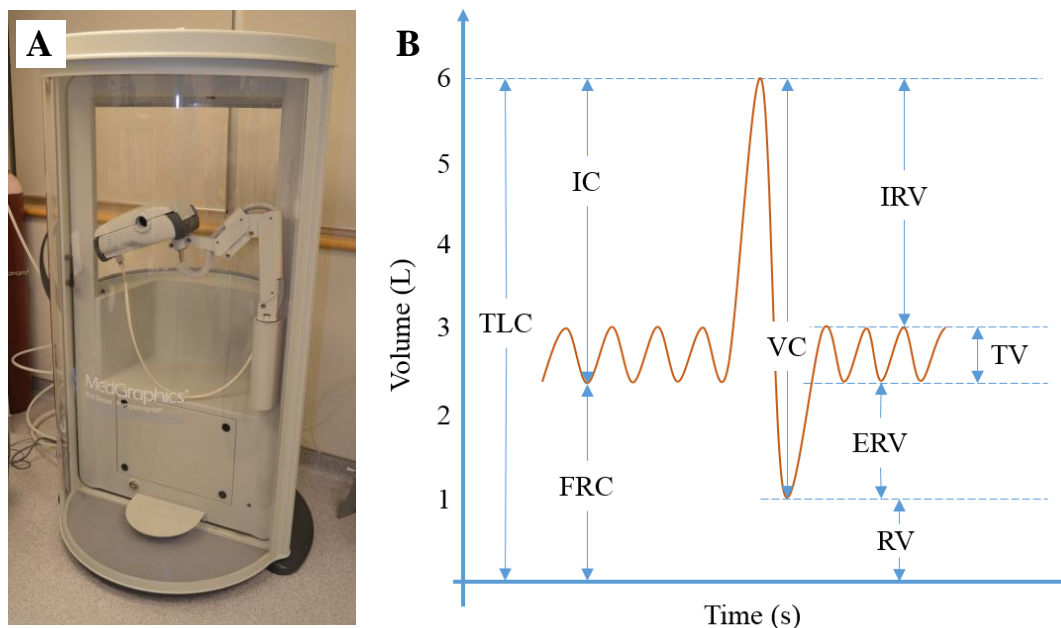
Figure 1-3: Static lung volumes. Panel A shows the body plethysmograph that is used in our laboratory. This device is used to measure static lung volumes shown in panel B based on Boyle's law. Panel B adapted from Respiratory Physiology.[24]

To measure gas exchange across the alveolar membrane, a third test which measures the diffusing capacity of carbon monoxide (DL_{CO}) can be used. During this maneuver, the subject is instructed to start with normal breathing. After a few normal breaths, the subject is instructed to blow all the way out until RV is reached, and then to breath in quickly. During the quick inspiration, the subject inhales a gas mixture with a low known concentration of carbon monoxide mixed with tracer gas, generally helium, and air. After a ten second breath hold the subject breathes out and the exhaled gas mixture is analyzed. Gas exchange is then calculated based on the difference in concentrations between the inhaled gases and alveolar gas sample.[19] All of the previously introduced measurements

of dynamic flow rates, static lung volumes and gas exchange are often expressed as a percent predicted value ($\%_{pred}$) which is calculated based on the gender, age, height and ethnicity of the individual being tested.[3, 25]

1.4.2   Six-minute walk distance

The six-minute walk distance (6MWD) is a test to assess exercise capacity according to guidelines set by the American Thoracic Society.[20] During this test the subject is asked to perform walking for six continuous minutes at a normal, comfortable pace along a flat corridor with a hard surface.[20] The Borg scale[26] is used to rate the breathlessness and overall physical fatigue before and after the test. Oxygen saturation (SpO_2) and heart rate are often recorded before and after the 6MWD test even though they are not a mandatory component. Previous studies have shown that 6MWD outcomes correlate well with morbidity and mortality.[27, 28]

1.4.3   Evaluating dyspnea and quality of life

As previously introduced, the mMRC[21] questionnaire has been developed to assess the level of dyspnea of an individual. The questionnaire ranks dyspnea on a level of Grade 0 ("I only get breathless with strenuous exercise") to Grade 4 ("I am too breathless to leave the house or I am breathless when dressing or undressing").[21, 29] Previous work has shown that the mMRC correlates well with 5-year mortality rates.[30] The SGRQ[22, 23] is another qualitative questionnaire developed for assessing overall quality of life in patients with obstructive airways disease. It evaluates symptoms, activities that relate to breathlessness and disturbance of daily life.[22] Each of the three topics are given a score ranging between zero and one hundred where a high score reflects a poor quality of life.[22]

1.5   COPD and Acute Exacerbations

1.5.1   Normal aging of the lung and COPD

As individuals age, like any other organ, the lung undergoes several important physiological changes. Previous work has shown that over time, there is a decrease in the

elastic recoil of the lung, a decrease in the compliance of the chest wall and a decrease in the strength of the respiratory muscle.[31] Furthermore, it has also been shown that individuals over 60 years of age can experience "senile emphysema", the homogeneous enlargement of airspaces without alveolar destruction or chronic inflammation.[32] Individuals with chronic obstructive pulmonary disease (COPD) experience an accelerated loss of lung function. As previously described COPD primarily affects our elderly population who have been exposed to tobacco smoke for extended periods of time.[3, 33] COPD is an inflammatory disease which can be broken down into two main conditions known as airways disease and emphysema. During airways disease, the walls of the airways are inflamed[34] and become thickened. Mucus secretion is increased, plugging the airways and leading to airway obstruction.[35, 36] During emphysema, the inflammatory response in the lung parenchyma causes destruction of lung tissue leading to alveolar enlargement.[36, 37] The current definition of emphysema set by the National Heart, Lung and Blood Institute states that emphysema is "a condition of the lung characterized by abnormal, permanent enlargement of airspaces distal to the terminal bronchiole, accompanied by the destruction of their walls and without obvious fibrosis".[38] Emphysema and airways disease are two separate conditions in COPD which can occur on their own or can coexist and the extent of each can vary amongst individuals. To diagnose COPD, spirometry is used where a post bronchodilator $FEV_1/FVC < 70\%$ indicates disease and disease severity is determined by the $FEV_1\%_{pred}$ score as outlined in Table 1-2.

Table 1-2 Spirometric classification of COPD

Stage	Severity	FEV_1 Criteria
GOLD 1:	mild	$FEV_1 \geq 80\%_{pred}$
GOLD 2:	moderate	$50\%_{pred} \leq FEV_1 < 80\%_{pred}$
GOLD 3:	severe	$30\%_{pred} \leq FEV_1 < 50\%_{pred}$
GOLD 4:	very severe	$FEV_1 < 30\%_{pred}$

Adapted from Vestbo et al.[39]

1.5.2   Acute exacerbations

As discussed above, COPD exacerbations are often experienced by individuals who are in moderate to severe stages of the disease. Guidelines set by the World Health Organization (WHO) and US National Heart Lung and Blood Institute Global Initiative for Chronic

Obstructive Lung disease (GOLD)[3] define a COPD exacerbations as: ''an event in the natural course of the disease characterized by a change in the patient's baseline dyspnea, cough, and/or sputum that is beyond normal day-to-day variations, is acute in onset, and may warrant a change in regular medication in a patient with underlying COPD".[3] It has been previously shown that the frequency of exacerbations increases with the severity of COPD. Frequency of exacerbations is an independent determinant of health-related patient quality of life.[40, 41] It has also been shown that exacerbations are associated with an increase in inflammatory markers that lead to accelerated disease progression.[42, 43] It is now believed that exacerbations are primarily triggered by viral and/or bacterial infections as well as air pollution.[44-47] Individuals are more prone to viral infections through the winter months and these types of infections tend to have longer recovery times than bacterial infections or those caused by air pollution.[48, 49] Current treatment for exacerbation depends on the severity of the event and is generally based on the clinical presentation of the patient.[50] Treatment includes use of short-acting β_2-agonist (such as salbutamol) and/or ipratropium MDI bronchodilators, corticosteroids such as prednisone, and antibiotics.[50-52] A previous study by Seemungal et al.[53] has shown that the median time for recovery from exacerbation symptoms is 7 (4 to 14) days; however there are a significant number of cases where full recovery to baseline values are not reached.[53] A different study demonstrated that patients who seek treatment sooner experience a faster recovery and report a higher health-related quality of life than those patients with more untreated exacerbations.[54] Evidence shows that about 50% of the exacerbations remain unreported[4, 40] which increases the risk for requiring an emergency hospitalization.[54] Aside from a decreased quality of life and increased morbidity of COPD patients, exacerbations also place a huge burden on the healthcare system. In Canada, the total cost for treating moderate and severe exacerbations including outpatient treatment, emergency department visits and hospitalization services is estimated to range from $646 to $736 million per year.[55] This amount is primarily attributed to hospitalizations which on average lasted 10 days and cost $8669 per individual.[55] A different study reported similar findings where the median hospital stay was reported to be 9 (5 to 15) days with a median cost of $7100 ($4100 to $16000) per individual.[56] Costs associated with treating moderate and severe exacerbations in the outpatient setting and emergency room are also significant and should

be considered. Treatment of moderate exacerbations in the outpatient setting and emergency room on average cost $126 and $515 per visit respectively.[55] Similarly, severe exacerbations cost $114 and $774 to treat in the outpatient setting and emergency room respectively.[55] Figure 1-4 outlines the cost breakdown for treating acute exacerbations, and as expected, hospitalizations account for the largest proportion of total cost[57].
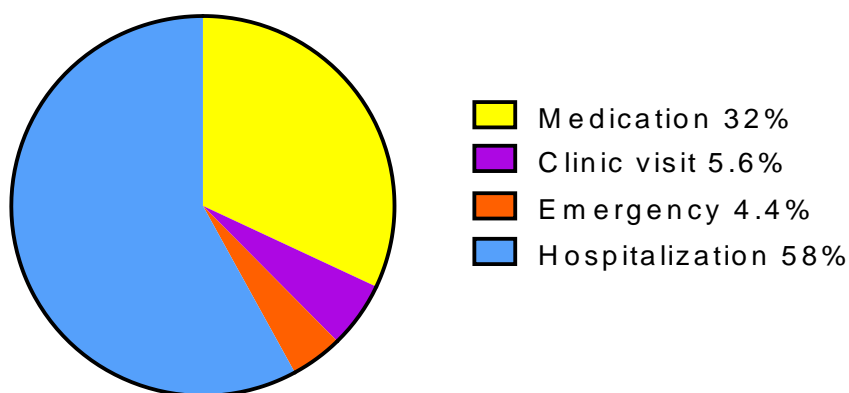
Figure 1-4: Exacerbation cost breakdown. This pie graph shows the costs attributed to treating COPD exacerbations. As expected, hospitalizations account for the largest proportion of total cost. Image adapted from Chapman et al[57]

Although frequency of exacerbations was shown to be related to a long-term decline in lung function[58], there are currently no widely available biomarkers able to predict the occurrence of these events. It has recently been shown that the single best predictor of acute exacerbations was the occurrence of previous exacerbations.[59] Therefore, there is need for new techniques that are able to predict the occurrence of these events for early detection and prevention of these episodes, as it would greatly improve patient quality of life, slow disease progression and decrease hospital costs associated with treatment. Decreasing costs attributed to hospitalization alone could halve the current costs required for treating COPD exacerbations.

Several studies have investigated preventive drugs that could potentially improve patient outcomes and reduce the number of hospitalizations. It has been shown that influenza vaccinations and treatment with immunostimulants may lower the number of exacerbations and are now recommended for individuals with COPD of significant severity.[44, 60-63] Long

acting bronchodilators (long-acting beta 2 agonist) such as salmeterol were shown to reduce the number of exacerbations over a 3-year period.[64] Pulmonary rehabilitation and self-management are also believed to reduce exacerbation risk. Evidence shows that exercise training can reduce the length of hospital stays following an exacerbation[54] and reduce the risk of being re-admitted.[65] Finally, long term oxygen therapy has also been shown to reduce the number of hospital admissions, in particular in hypoxaemic COPD individuals.[66]

1.6 Imaging Lung Function and Structure

1.6.1 X-ray Computed Tomography

Plane X-rays were introduced in 1895 as an important imaging modality. However, the projection nature of these images limits their use.[67] Computed tomography (CT) utilizes X-rays to form two dimensional cross-sectional images of the body.[67] While Nobel Prize recipients G.N. Hounsfield and A.M. Cormack introduced the clinical significance of CT in 1972, much of this work relied on theoretical work by J.H. Radon in 1917 and Bernard Ziedses des Plantes in 1931.[67] The first CT scanner was intended for imaging of the brain, but its use was later extended to many different applications with the development of the whole body CT scanner in 1975. CT imaging utilizes X-ray transmission profiles captured under a number of different angles through cross sections of the body.[67] To capture multiple transmission profiles, an X-ray source and detectors are mounted on a gantry which rotates around the patient.[67] First generation CT scanners acquired multiple X-ray profiles for each cross sectional image by rotating 360 degrees around the patient.[67] Then the patient would be shifted a short distance by moving the table so that the next slice could be captured.[67] The rotation of the gantry was limited by wires attached to the instrumentation on the gantry. Modern CT scanners have an improved design, such that the gantry can rotate an unlimited number of times in the same direction. With this improvement, spiral CT was developed where the patient is translated through the bore of the gantry while transmission profiles are captured.[67] Modern CT scanners also utilize multi-slice detectors along with a fan shaped X-ray beam, allowing for multiple transmission profiles to be recorded simultaneously, significantly decreasing acquisition time and allowing for whole body imaging within a single breath-hold.[67] The CT scanner

used to capture images for our studies consists of a 64 slice array of detectors. Panel A of Figure 1-5 represents the acquisition pattern of a spiral acquisition, while panel B demonstrates the multi-slice aspect of the acquisition.
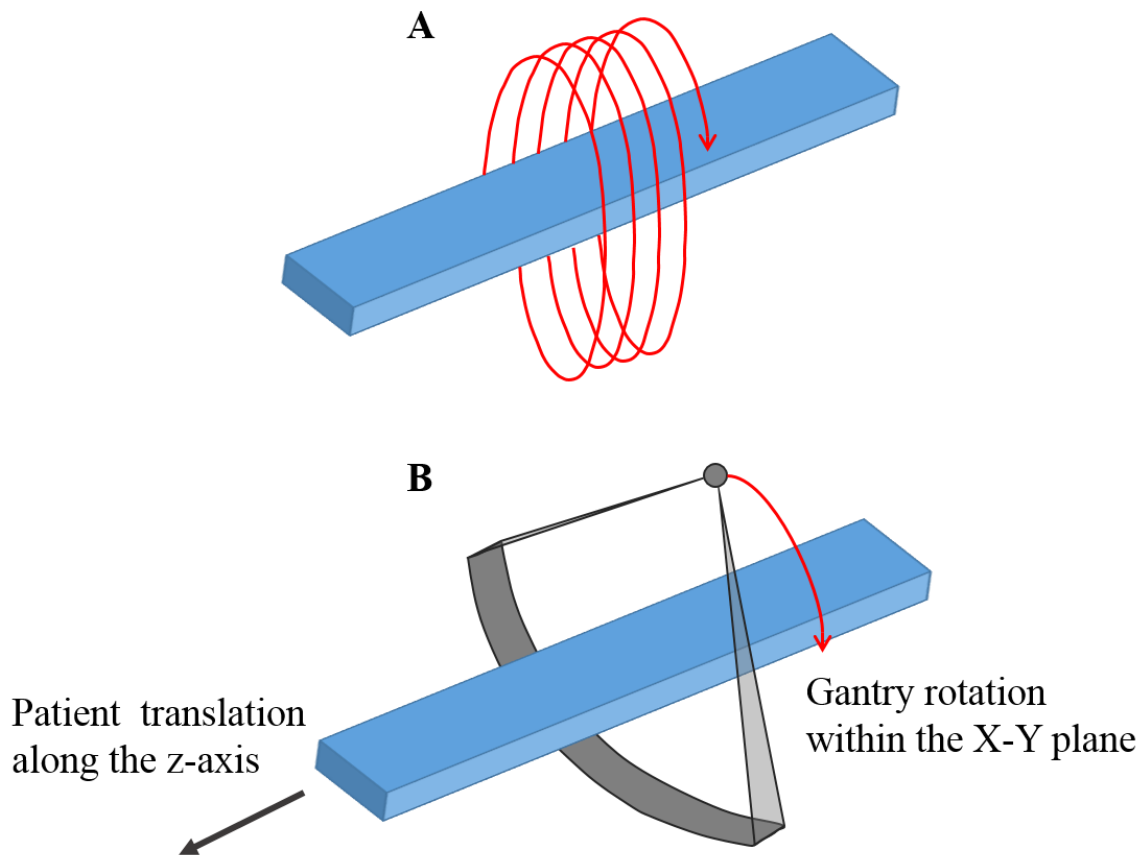
Figure 1-5: CT acquisition. The subject is translated through the bore of the gantry while the X-ray source and the detectors attached to the gantry rotate freely around the subject. Panel A shows the spiral acquisition resulting from this process. Panel B depicts the concept of a fan shaped X-ray beam and detectors spanning multiple slices. Image adapted from Castellano et al.[67]

Images are reconstructed by intensive mathematical computations, known as filtered back projections, of the measured transmission profiles.[68] The pixel intensities in the reconstructed image are determined based on the corresponding linear attenuation coefficients of tissues (μ_{tissue}) in the body and are measured in Hounsfield units (HU). As

shown in Equation 3, Hounsfield values are normalized to the linear attenuation coefficient of water, thus water has a value of 0HU. By definition, air is -1000HU, lung is from -600HU to -950HU, fat is from -60HU to -80HU, soft tissue is from 20HU to 70HU and bone is 1000HU or higher.

$$HU = \frac{\mu_{tissue} - \mu_{water}}{\mu_{water}} \times 1000 \qquad (3)$$

Important parameters that are considered when acquiring an image are the rotation time, which is the amount of time taken by the gantry to complete a single revolution; the tube voltage; the tube current, which is generally limited by overheating of the X-ray tube and the scan time; and, the pitch, which is the ratio of table translation per 360 degrees of tube rotation relative to the beam width. All of these factors are optimized such that images of sufficient diagnostic quality are achieved while limiting the ionizing radiation that the patient is exposed to.

Computed tomography is the imaging method of choice for lung imaging as it allows for the visualization of airways and parenchyma.[69-72] Emphysematous lesions in the lung parenchyma have lower tissue densities than healthy lung tissue and can be identified by regions of lower attenuation values, in Hounsfield units, on density frequency histograms.[71, 73] The extent of emphysema can be evaluated using a thresh-hold cut-off value; the voxels below this value are characterized as emphysematous tissue. A commonly used cut-off is -950 HU, where tissues with attenuation values below -950 HU are characterized as emphysema.[74]

Airway remodeling in COPD is primarily caused by inflammation in the epithelium of the airway wall and mucus plugs in the airway lumen.[36] Therefore, airways disease severity can also be evaluated using computed tomography by obtaining dimensions of the airway wall area and lumen area.[75] These measurements are challenging since airway inflammation primarily affects the small airways (<2mm in diameter)[35], which are difficult to visualize using CT.[73, 76]

1.6.2 Magnetic resonance imaging

Conventional proton magnetic resonance imaging (^{1}H MRI) has become a widely used medical imaging modality which relies on the presence of water- and fat- bound hydrogen (^{1}H) atoms in the body to acquire images.[77] However, due to the relatively low ^{1}H density present in the lungs, as shown in Figure 1-6A, the thoracic cavity appears black on conventional ^{1}H images, providing little morphological information about the lungs.[77] This limitation has triggered the development of new MRI techniques for visualizing lung function and structure. In particular, the development of hyperpolarized noble gas imaging has emerged as a useful technique for imaging the lungs.[73, 78] Breath-hold imaging after inhalation of hyperpolarized helium-3 (^{3}He) allows for visualization of gas distribution within the lungs.[77] These images are known as static ventilation images and examples are shown in Figures 1-6B and C. Figure 1-6B represents a healthy adult where after inhalation of ^{3}He the signal is homogeneously distributed throughout the lungs. A homogeneous signal distribution suggests that all areas of the lung have a homogeneous gas distribution.
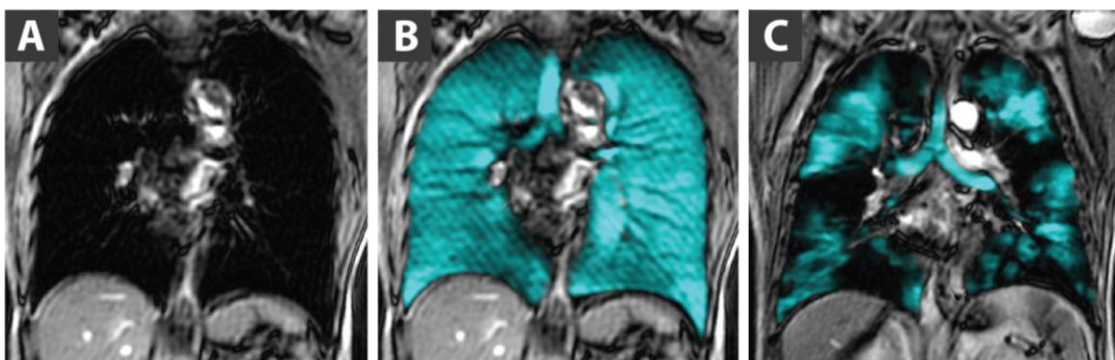
Figure 1-6: Proton and hyperpolarized helium-3 MRI of lung. Panel A shows proton image of lungs. Panel B shows hyperpolarized helium-3 (^{3}He) MRI overlaid on proton MRI for a healthy individual; the inhaled gas is homogeneously distributed in the lungs. Panel C shows ^{3}He MRI static ventilation image overlaid on proton MRI for an individual with COPD. Areas of signal void in the image represent ventilation defects in the lung.

In contrast, Figure 1-6C shows the signal distribution for an individual with COPD, with regions of signal void, known as ventilation defects. These areas are indicative of poorly ventilated or completely unventilated regions in the lung. Quantitative measurements of

ventilation defects have been developed, such as ventilation defect volume (VDV)[79] and ventilation defect percent (VDP)[80] by normalizing static ventilation images to the thoracic cavity volume obtain using ^{1}H MRI. The etiology of ventilation defects is still unclear. It is believed that in COPD they may be due to airway disease, emphysema or a combination of both diseases.[73] It is also possible that ventilation defects are slow filling regions of the lung, relative to the breath-hold scan.

^{3}He MRI has also been used for evaluating the microstructure of the lungs. Diffusion weighted ^{3}He MRI imaging allows for characterization of alveolar size.[81-83] By generating apparent diffusion coefficient (ADC) maps, alveolar destruction in emphysema can be quantified, where higher ADC values represent larger alveolar spaces and therefore greater disease severity.[82] Higher ADC values are generated for diseased individuals, because the gas atoms travel further per unit time.[73] Figure 1-7 depicts ADC maps for a healthy subject and an individual with COPD where the severity of disease is represented by brighter colours.
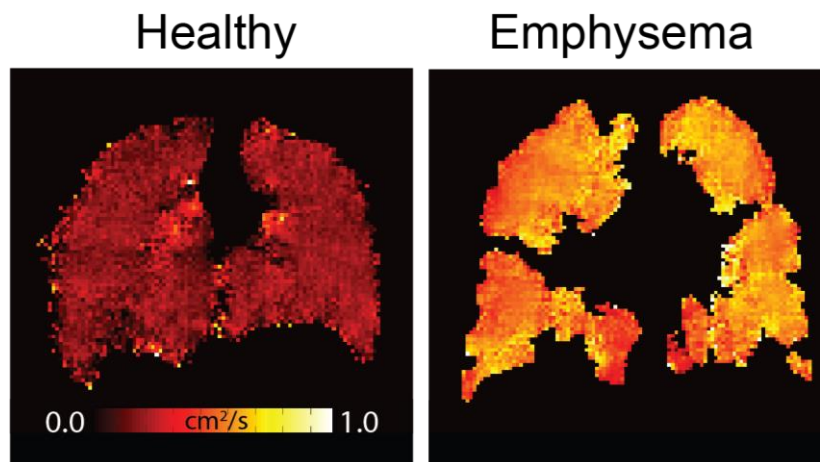
Figure 1-7: Apparent diffusion coefficient (ADC) maps. Left panel represents a healthy individual while right panel represents an individual with emphysema. Brighter colour represents higher ADC values.

1.7 The Pulmonary Arteries

The cardiovascular system can be divided into two components, the systemic circulation which includes blood delivery between the heart and the organs and tissues in the body, and the pulmonary circulation which includes blood delivery between the heart and the lungs for re-oxygenation and waste removal.[84] The pulmonary arteries (PA) make up the first component of the pulmonary circulation. They are responsible for delivering oxygen-poor blood from the right ventricle of the heart to the lungs so that it can become re-oxygenated.[85] As shown in Figure 1-8, the main pulmonary artery or the pulmonary trunk, leads from the right ventricle of the heart and it divides into the left and right pulmonary arteries, supplying the left and right lung respectively.
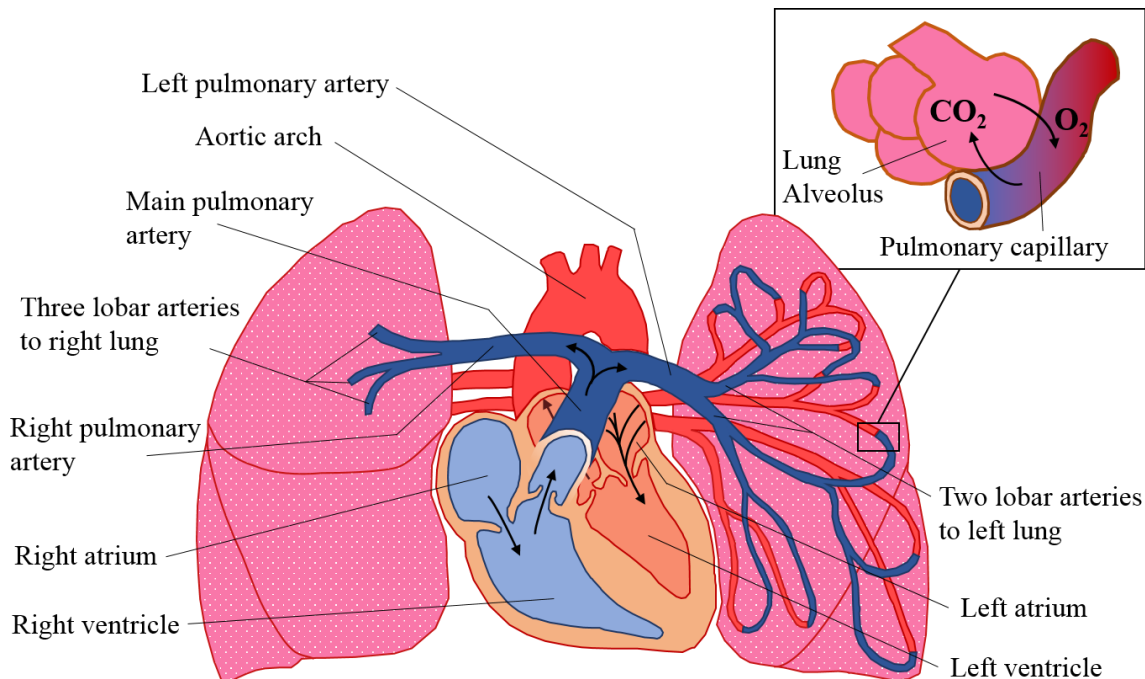
Figure 1-8: Pulmonary circulation. Black arrows represent the direction of blood flow in the heart. De-oxygenated blood leaves the right ventricle of the heart through the main pulmonary artery (PA). The main PA then divides into the right and left PAs which then divide into three and two lobar arteries respectively. Arteries continue to branch along with the airway tree. Gas exchange occurs in the pulmonary capillaries where diffusion allows carbon dioxide (CO_2) to be removed from the blood and for blood to get re-oxygenated. Oxygenated blood returns to the heart to be transported to the systemic circulation. Image adapted from Marieb EN, Human Anatomy.[85]

Each PA then divides into lobar arteries to supply the three lobes of the right and the two lobes of the left lung.[85] The arteries continue dividing, along with the bronchi and bronchioles in the lung, becoming arterioles, and finally pulmonary capillaries at the level of the alveoli where most gas exchange occurs. As previously described, gas exchange occurs as determined by Fick's law of diffusion outlined in Equation 1.

As shown in Figure 1-9, the walls of the pulmonary arteries are assembled from three main layers, each of which have a different composition. The layer closest to the lumen is called the tunica intima layer and is made up of endothelial cells as well as a thin layer of connective elastic tissue.[17] The composition of the next layer, known as the tunica media, changes as the size of the artery becomes smaller. Larger arteries have media layers made of connective elastic tissue, while smaller vessels have media layers made up of smooth muscle.[17] The smallest arterioles in the pulmonary circulation however, do not have a detectable smooth muscle media layer.[86] The tunica adventitia is the outermost layer of the artery and is made up of connective tissue. Smaller vessels present in this layer provide nutrients for all three layers of the artery.[17]
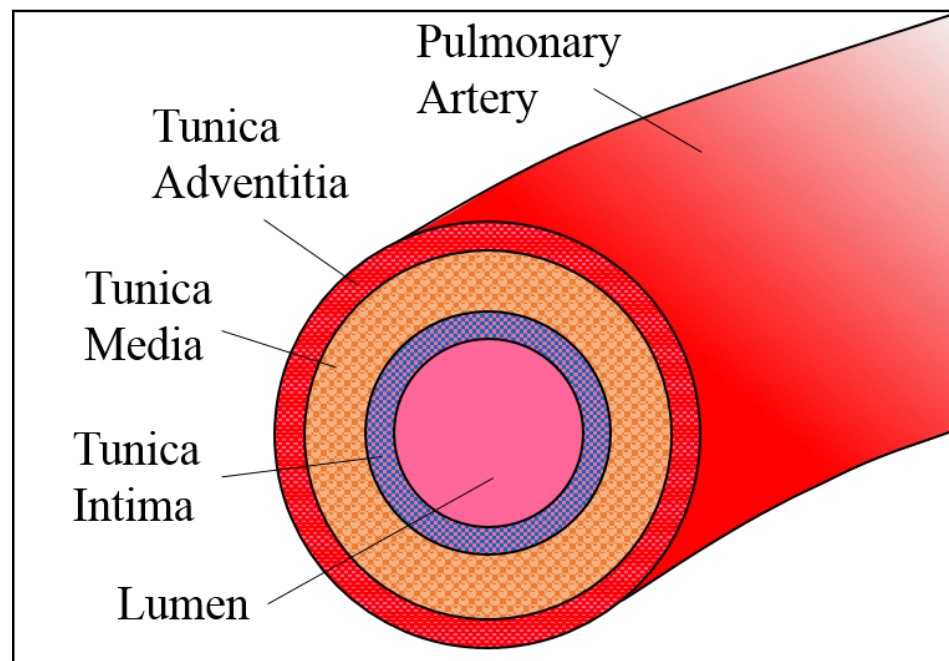
Figure 1-9: Layers of pulmonary artery walls. The three main layers that compose the walls of pulmonary arteries are the tunica intima, tunica media and tunica adventitia moving from the lumen towards the outside of the vessel.

1.8 Imaging pulmonary artery abnormalities

Cardiovascular disease is an important risk factor in individuals with COPD. Evidence shows that it is the single largest cause of hospitalizations and the leading cause of death, following lung cancer.[9, 10] Specifically, pulmonary vascular disease has been associated with exacerbation related hospitalizations as well as mortality.[87-89] A common condition is the enlargement of the pulmonary artery (PA) trunk and often the right ventricle of the heart. It is believed that in order to re-direct blood-flow to well ventilated regions of the lung, hypoxic arteriolar vasoconstriction increases the resistance of the pulmonary vasculature, increasing the pressure in the PA trunk and in the right ventricle of the heart.[90] This increase in pressure leads to an enlarged pulmonary artery and a condition known as pulmonary hypertension (PH).[90] Currently the gold standard for monitoring PH is through right heart catheterization; however, this is an invasive technique and can cause discomfort.[11] The invasiveness of this technique makes it unsuitable for performing repeated measurements and therefore unsuitable for evaluating disease progression and treatment response. Therefore, several studies have sought to estimate pulmonary hypertension by evaluating pulmonary artery abnormalities using non-invasive imaging techniques. In the following subsections I will discuss different imaging modalities that have been considered for evaluating the size of the pulmonary artery.

1.8.1 Imaging PA using Doppler echocardiography

Doppler echocardiography is the most common imaging technique for evaluating individuals at risk of pulmonary hypertension.[91] This non-invasive technique measures the peak velocity of the regurgitant jet through the tricuspid valves.[91] However, numerous studies have explored the relationship between echocardiography and pulmonary artery pressures measured using right heart catheterization and have reported poor correlations between these techniques.[91-94] Therefore, right heart catheterization remains the gold standard for evaluating pulmonary hypertension and different imaging approaches have been proposed.

1.8.2   Imaging PA using plane X-rays

Pulmonary artery enlargement was first evaluated on X-ray images[95-98]; however, this technique was limited in predicting PH due to the projection nature of plane radiographs.[99] Therefore, these studies relied on measuring the width of the right pulmonary artery to evaluate its size as it is situated lateral to the right lower lobe bronchus and is generally well distinguished on radiographs.[100] However, in cases where the heart is dilated beyond the right lower lobe bronchus, the right pulmonary artery is no longer well visible on plane radiographs and is more difficult to evaluate.[100] Teichmann et al. measured right pulmonary artery diameters in 112 healthy individuals as well as 95 men suffering from chronic bronchitis.[96] They showed that PH could be diagnosed using the width of the right pulmonary artery with a reliability of 72.2% in readable films, which dropped to 64.2% when including films which were not reliably readable.[96] The limitation of plane radiographs triggered further research in measuring PA size with the development of x-ray computed tomography.

1.8.3   Imaging PA using X-ray computed tomography

The limitation of plane X-ray radiographs was overcome by the discovery of X-ray computed tomography. With advances in CT imaging, several studies have revisited the relationship between PA size and pulmonary hypertension to determine whether it would provide a suitable non-invasive means of assessing patients at risk. These studies have reported a positive correlation between main pulmonary artery diameter and pulmonary artery pressure measured using right heart catheterization.[11, 99, 101-105] In particular, Lange et al. demonstrated that the diameter of the main pulmonary artery measured on chest CT images could potentially be used as a biomarker for predicting borderline pulmonary hypertension.[11] Furthermore, recent findings by Wells et al. suggested that a PA to aorta (A) diameter ratio of greater than 1 (PA/A > 1), as measured on chest CT images, was significantly associated with a history of acute exacerbations, as well as with risk factors of future exacerbations.[1] Figure 1-10 shows a representative measurement of the main pulmonary artery (MPA) and aorta diameter.
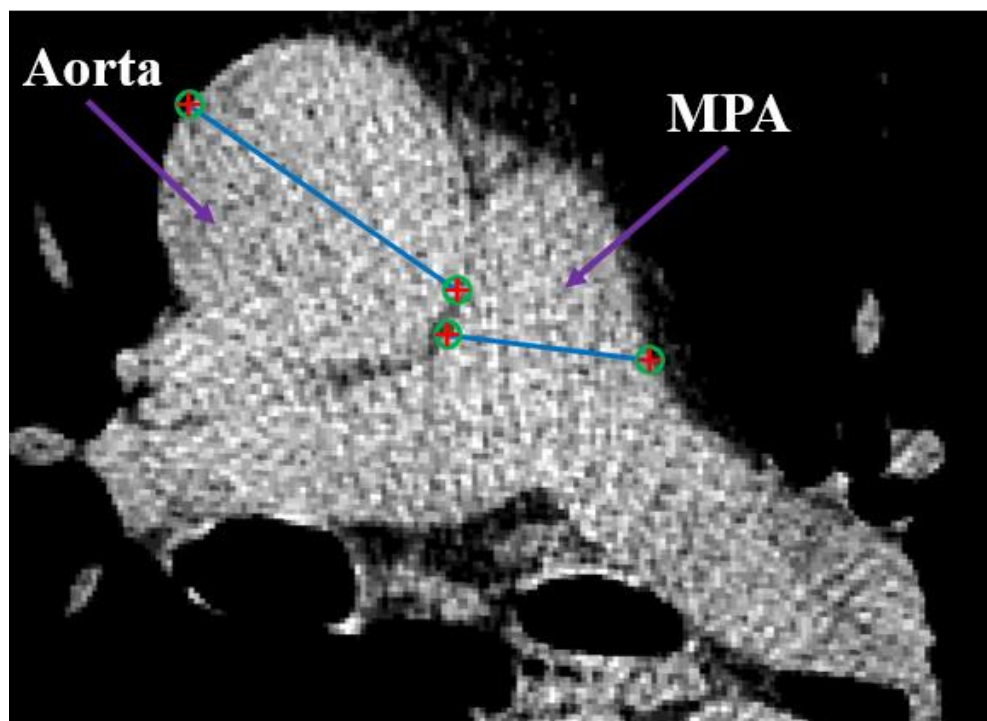
Figure 1-10: Pulmonary artery diameter measurement. Main pulmonary artery (MPA) and aorta diameter measurement at the level of the bifurcation. Adapted from Wells et al.[1]

1.8.4 Evaluating PA abnormalities with magnetic resonance imaging

Several non-invasive, magnetic resonance imaging (MRI) techniques have been developed to estimate pulmonary hypertension, including evaluation of pulmonary artery size.[106-110] Frank et al. found significantly greater main pulmonary artery diameters measured on MRI images in 23 hypertensive individuals when compared to a control group (n = 8).[106] Furthermore, Saba et al. showed that the ventricular mass index (ratio of right ventricular mass over left ventricular mass) was associated with pulmonary artery pressures measured by right heart catheterization.[107] Additionally, Tardivon et al. found that in a group of 13 pulmonary hypertensive individuals, acceleration time (the time from the onset of forward flow to the moment of maximum flow velocity in the main pulmonary artery) was strongly correlated with pulmonary artery pressure measured using right heart catheterization.[108] Similar results were found by Wacker et al. in a group of 12 hypertensive patients.[109] Finally, Marcus et al. showed a correlation between systolic pulmonary artery pressure and acceleration time/ejection time ratio in a group of 12 patients.[110]

1.9   Emerging tools for quantifying pulmonary artery size

As previously described, current methods for quantifying the size of the pulmonary artery rely on a simple one-dimensional diameter measurement of the main PA to assess morphological changes of the PA. However a one-dimensional measurement may not be sufficient to fully encompass three-dimensional changes of the vessel.   Therefore additional research is required to develop more accurate techniques for quantifying the size of the PA that would encompass changes of the artery in three dimensions.   Chapter two of this thesis describes a three-dimensional method that we developed for quantifying the size of the pulmonary artery from thoracic computed tomography images.   It consists of a slice-by-slice manual segmentation of each of the main, left and right pulmonary arteries in planes perpendicular to the axis of each vessel.

1.10 Research Hypothesis and Objectives

As previously described, acute exacerbations of COPD are of major concern because they reduce patients' health-related quality of life and increase patients' morbidity and mortality. They also account for a large portion of healthcare costs, placing a large burden on our healthcare system. Currently there are no widely available biomarkers that are able to accurately predict the occurrence of these events. Previous work[1] investigated the use of a one-dimensional diameter measurement of the main pulmonary artery to evaluate patients' exacerbation risk. However, we believe that a three-dimensional approach would be more appropriate for quantifying morphological changes in the pulmonary artery as it would account for changes in all three Cartesian planes of the vessel. Therefore, the primary objectives of this thesis were: 1) to develop a three-dimensional measurement for assessing the size of the pulmonary artery and test the observer reproducibility and 2) to assess the association between pulmonary artery volume and COPD, as well as exacerbation frequency. The purpose of these objectives was to develop a quick and easy-to-use biomarker that could help improve health-related patient quality of life and reduce hospital costs.

In Chapter 2, our objective was to develop a three-dimensional volumetric measurement technique to quantify the size of the main, left and right pulmonary arteries at the level of

their bifurcation. Three observers performed five rounds of repeated measurements to evaluate reproducibility. We hypothesized that measurements will be reproducible with low inter- and intra-observer variability as well as with low longitudinal variability.

In Chapter 3, we investigated the relationship between pulmonary artery volume measurements and measurements of lung function and structure in a group of ex-smokers. Pulmonary artery volumes of these individuals were also compared to those measured in a group of never-smokers. We also investigated the potential use of our technique as a suitable biomarker for predicting the occurrence of severe exacerbations of COPD. We hypothesized that pulmonary artery volumes will be associated with measurements of lung function and structure. Furthermore, we hypothesized that pulmonary artery volumes will be able to predict the occurrence of COPD exacerbations.

1.11 References

[1] Wells JM, Washko GR, Han MK, et al. Pulmonary arterial enlargement and acute exacerbations of COPD. New England Journal of Medicine 2012;367(10):913-21.

[2] Kirby M, Owrangi A, Svenningsen S, et al. On the role of abnormal DLCO in ex-smokers without airflow limitation: symptoms, exercise capacity and hyperpolarised helium-3 MRI. Thorax 2013;68(8):752-9.

[3] Rabe KF, Hurd S, Anzueto A, et al. Global strategy for the diagnosis, management, and prevention of chronic obstructive pulmonary disease: GOLD executive summary. American journal of respiratory and critical care medicine 2007;176(6):532-55.

[4] Burge S, Wedzicha J. COPD exacerbations: definitions and classifications. European Respiratory Journal 2003;21(41 suppl):46s-53s.

[5] Chae EJ, Seo JB, Oh Y-M, Lee JS, Jung Y, Do Lee S. Severity of Systemic Calcified Atherosclerosis Is Associated With Airflow Limitation and Emphysema. Journal of computer assisted tomography 2013;37(5):743-9.

[6] Dransfield MT, Huang F, Nath H, Singh SP, Bailey WC, Washko GR. CT emphysema predicts thoracic aortic calcification in smokers with and without COPD. COPD: Journal of Chronic Obstructive Pulmonary Disease 2010;7(6):404-10.

[7] McAllister DA, MacNee W, Duprez D, et al. Pulmonary function is associated with distal aortic calcium, not proximal aortic distensibility. MESA lung study. COPD: Journal of Chronic Obstructive Pulmonary Disease 2011;8(2):71-8.

[8] Rasmussen T, Køber L, Pedersen JH, et al. Relationship between chronic obstructive pulmonary disease and subclinical coronary artery disease in long-term smokers. European Heart Journal–Cardiovascular Imaging 2013;14(12):1159-66.

[9] Anthonisen NR, Skeans MA, Wise RA, Manfreda J, Kanner RE, Connett JE. The Effects of a Smoking Cessation Intervention on 14.5-Year MortalityA Randomized Clinical Trial. Annals of internal medicine 2005;142(4):233-9.

[10] Sidney S, Sorel M, Quesenberry CP, DeLuise C, Lanes S, Eisner MD. COPD and incident cardiovascular disease hospitalizations and mortality: Kaiser Permanente Medical Care Program. CHEST Journal 2005;128(4):2068-75.

[11] Lange TJ, Dornia C, Stiefel J, et al. Increased pulmonary artery diameter on chest computed tomography can predict borderline pulmonary hypertension. Pulmonary circulation 2013;3(2):363.

[12] WHO. The global burden of disease: 2004 update. In:

[13] WHO. The top 10 causes of death. In, 2014

[14] WHO. World Health Statistics. In, 2008

[15] Davies AS, Moores C, Britton R. The Respiratory System. Churchill Livingstone, 2003.

[16] West JB. Respiratory Physiology: The Essentials. Wolters Kluwer Health/Lippincott Williams & Wilkins, 2012.

[17] Jardins TRD. Cardiopulmonary Anatomy & Physiology: Essentials for Respiratory Care. Delmar/Thomson Learning, 2002.

[18] Aykac D, Hoffman EA, McLennan G, Reinhardt JM. Segmentation and analysis of the human airway tree from three-dimensional X-ray CT images. Medical Imaging, IEEE Transactions on 2003;22(8):940-50.

[19] Light RW. Chest Medicine: Essentials of Pulmonary and Critical Care Medicine. Lippincott Williams & Wilkins, 2005.

[20] Laboratories ACoPSfCPF. ATS statement: guidelines for the six-minute walk test. American Journal of Respiratory and Critical Care Medicine 2002;166(1):111.

[21] Global Strategy for the Diagnosis MaPoC. Global Initiative for Chronic Obstructive Lung Disease (GOLD) 2014. In, 2014

[22] Cotes JE, Chinn DJ, Miller MR. Lung Function: Physiology, Measurement and Application in Medicine. Wiley, 2009.

[23] Jones PW, Quirk FH, Baveystock CM, Littlejohns P. A self-complete measure of health status for chronic airflow limitation: the St. George's Respiratory Questionnaire. American Review of Respiratory Disease 1992;145(6):1321-7.

[24] Balfour SN. Respiratory Physiology. The C.V. Mosby Company, 1987.

[25] Clayton N. Review Series: Lung function made easy: Assessing lung size. Chronic respiratory disease 2007;4(3):151-7.

[26] Borg GA. Psychophysical bases of perceived exertion. Med sci sports exerc 1982;14(5):377-81.

[27] Pinto-Plata V, Cote C, Cabral H, Taylor J, Celli B. The 6-min walk distance: change over time and value as a predictor of survival in severe COPD. European Respiratory Journal 2004;23(1):28-33.

[28] Casanova C, Cote C, Marin JM, et al. Distance and oxygen desaturation during the 6-min walk test as predictors of long-term mortality in patients with COPD. CHEST Journal 2008;134(4):746-52.

[29] Mahler D, Wells CK. Evaluation of clinical methods for rating dyspnea. CHEST Journal 1988;93(3):580-6.

[30] Nishimura K, Izumi T, Tsukino M, Oga T. Dyspnea is a better predictor of 5-year survival than airway obstruction in patients with COPD. CHEST Journal 2002;121(5):1434-40.

[31] Janssens J, Pache J, Nicod L. Physiological changes in respiratory function associated with ageing. European Respiratory Journal 1999;13(1):197-205.

[32] Verbeken E, Cauberghs M, Mertens I, Clement J, Lauweryns J, Van de Woestijne K. The senile lung. Comparison with normal and emphysematous lungs. 1. Structural aspects. CHEST Journal 1992;101(3):793-9.

[33] Pauwels R, Buist AS, Calverley PA, Jenkins C, Hurd S. Global Strategy for the Diagnosis, Management, and Prevention of Chronic Obstructive Pulmonary Disease. American Journal of Respiratory and Critical Care Medicine 2001;163(5):1256-76.

[34] Mullen J, Wright JL, Wiggs BR, Pare PD, Hogg JC. Reassessment of inflammation of airways in chronic bronchitis. British medical journal (Clinical research ed) 1985;291(6504):1235.

[35] Hogg JC, Chu F, Utokaparch S, et al. The nature of small-airway obstruction in chronic obstructive pulmonary disease. New England Journal of Medicine 2004;350(26):2645-53.

[36] Hogg JC. Pathophysiology of airflow limitation in chronic obstructive pulmonary disease. The Lancet 2004;364(9435):709-21.

[37] Finkelstein R, Fraser RS, Ghezzo H, Cosio MG. Alveolar inflammation and its relation to emphysema in smokers. American journal of respiratory and critical care medicine 1995;152(5):1666-72.

[38] Snider G. The definition of emphysema; report of a National Heart, Lung and Blood Institute. Division of Lung Diseases. Workshop. Am Rev Respir Dis 1985;132:182-5.

[39] Vestbo J, Hurd SS, Agusti AG, et al. Global strategy for the diagnosis, management, and prevention of chronic obstructive pulmonary disease: GOLD executive summary. American journal of respiratory and critical care medicine 2013;187(4):347-65.

[40] Seemungal TA, Donaldson GC, Paul EA, Bestall JC, Jeffries DJ, Wedzicha JA. Effect of exacerbation on quality of life in patients with chronic obstructive pulmonary disease. American journal of respiratory and critical care medicine 1998;157(5):1418-22.

[41] Reilly JJ. Stepping down therapy in COPD. New England Journal of Medicine 2014;371(14):1340-1.

[42] Bhowmik A, Seemungal TA, Sapsford RJ, Wedzicha JA. Relation of sputum inflammatory markers to symptoms and lung function changes in COPD exacerbations. Thorax 2000;55(2):114-20.

[43] Perera WR, Hurst JR, Wilkinson TM, et al. Inflammatory changes, recovery and recurrence at COPD exacerbation. European Respiratory Journal 2007;29(3):527-34.

[44] Wedzicha JA, Seemungal TA. COPD exacerbations: defining their cause and prevention. The Lancet 2007;370(9589):786-96.

[45] Anderson HR, Limb ES, Bland JM, De Leon AP, Strachan DP, Bower JS. Health effects of an air pollution episode in London, December 1991. Thorax 1995;50(11):1188-93.

[46] Anderson H, Spix C, Medina S, et al. Air pollution and daily admissions for chronic obstructive pulmonary disease in 6 European cities: results from the APHEA project. European respiratory journal 1997;10(5):1064-71.

[47] Yang C-Y, Chen C-J. Air pollution and hospital admissions for chronic obstructive pulmonary disease in a subtropical city: Taipei, Taiwan. Journal of Toxicology and Environmental Health, Part A 2007;70(14):1214-9.

[48] Hurst J, Donaldson G, Wilkinson T, Perera W, Wedzicha J. Epidemiological relationships between the common cold and exacerbation frequency in COPD. European Respiratory Journal 2005;26(5):846-52.

[49] Seemungal T, Harper-Owen R, Bhowmik A, Jeffries D, Wedzicha J. Detection of rhinovirus in induced sputum at exacerbation of chronic obstructive pulmonary disease. European Respiratory Journal 2000;16(4):677-83.

[50] Celli B, MacNee W, Agusti A, et al. Standards for the diagnosis and treatment of patients with COPD: a summary of the ATS/ERS position paper. European Respiratory Journal 2004;23(6):932-46.

[51] Seemungal TA, Hurst JR, Wedzicha JA. Exacerbation rate, health status and mortality in COPD–a review of potential interventions. International journal of chronic obstructive pulmonary disease 2009;4:203.

[52] Anthonisen NR, Manfreda J, Warren C, Hershfield E, Harding G, Nelson N. Antibiotic therapy in exacerbations of chronic obstructive pulmonary disease. Annals of internal medicine 1987;106(2):196-204.

[53] Seemungal TA, Donaldson GC, Bhowmik A, Jeffries DJ, Wedzicha JA. Time course and recovery of exacerbations in patients with chronic obstructive pulmonary

disease. American journal of respiratory and critical care medicine 2000;161(5):1608-13.

[54] Wilkinson TM, Donaldson GC, Hurst JR, Seemungal TA, Wedzicha JA. Early therapy improves outcomes of exacerbations of chronic obstructive pulmonary disease. American journal of respiratory and critical care medicine 2004;169(12):1298-303.

[55] Mittmann N, Kuramoto L, Seung S, Haddon J, Bradley-Kennedy C, Fitzgerald J. The cost of moderate and severe COPD exacerbations to the Canadian healthcare system. Respiratory medicine 2008;102(3):413-21.

[56] Connors Jr AF, Dawson NV, Thomas C, et al. Outcomes following acute exacerbation of severe chronic obstructive lung disease. The SUPPORT investigators (Study to Understand Prognoses and Preferences for Outcomes and Risks of Treatments). American journal of respiratory and critical care medicine 1996;154(4):959-67.

[57] Chapman K, Mannino DM, Soriano J, et al. Epidemiology and costs of chronic obstructive pulmonary disease. European Respiratory Journal 2006;27(1):188-207.

[58] Donaldson G, Seemungal T, Bhowmik A, Wedzicha J. Relationship between exacerbation frequency and lung function decline in chronic obstructive pulmonary disease. Thorax 2002;57(10):847-52.

[59] Hurst JR, Vestbo J, Anzueto A, et al. Susceptibility to exacerbation in chronic obstructive pulmonary disease. New England Journal of Medicine 2010;363(12):1128-38.

[60] Nichol KL, Baken L, Nelson A. Relation between influenza vaccination and outpatient visits, hospitalization, and mortality in elderly persons with chronic lung disease. Annals of internal medicine 1999;130(5):397-403.

[61] Gorse GJ, O'Connor TZ, Young SL, et al. Impact of a winter respiratory virus season on patients with COPD and association with influenza vaccination. CHEST Journal 2006;130(4):1109-16.

[62] Wongsurakiat P, Maranetra KN, Wasi C, Kositanont U, Dejsomritrutai W, Charoenratanakul S. Acute Respiratory Illness in Patients With COPD and the Effectiveness of Influenza VaccinationA Randomized Controlled Study. CHEST Journal 2004;125(6):2011-20.

[63] Wang C-S, Wang S-T, Lai C-T, Lin L-J, Chou P. Impact of influenza vaccination on major cause-specific mortality. Vaccine 2007;25(7):1196-203.

[64] Calverley PM, Anderson JA, Celli B, et al. Salmeterol and fluticasone propionate and survival in chronic obstructive pulmonary disease. New England Journal of Medicine 2007;356(8):775-89.

[65] Garcia-Aymerich J, Farrero E, Felez M, Izquierdo J, Marrades R, Anto J. Risk factors of readmission to hospital for a COPD exacerbation: a prospective study. Thorax 2003;58(2):100-5.

[66] Ringbaek T, Viskum K, Lange P. Does long-term oxygen therapy reduce hospitalisation in hypoxaemic chronic obstructive pulmonary disease? European Respiratory Journal 2002;20(1):38-42.

[67] Castellano I, Geleijns J. COMPUTED TOMOGRAPHY. In: Lemoigne Y, Caner A, Rahal G, editors. Physics for Medical Imaging Applications: Springer Netherlands, 2007: 367-79

[68] Kak AC, Slaney M. Principles of Computerized Tomographic Imaging. Society for Industrial and Applied Mathematics, 1988.

[69] Coxson HO, Rogers RM. Quantitative Computed Tomography of Chronic Obstructive Pulmonary Disease 1. Academic radiology 2005;12(11):1457-63.

[70] Mets O, De Jong P, Van Ginneken B, Gietema H, Lammers J. Quantitative computed tomography in COPD: possibilities and limitations. Lung 2012;190(2):133-45.

[71] Coxson HO, Mayo J, Lam S, Santyr G, Parraga G, Sin DD. New and current clinical imaging techniques to study chronic obstructive pulmonary disease. American journal of respiratory and critical care medicine 2009;180(7):588-97.

[72] Matsuoka S, Yamashiro T, Washko GR, Kurihara Y, Nakajima Y, Hatabu H. Quantitative CT Assessment of Chronic Obstructive Pulmonary Disease 1. Radiographics 2010;30(1):55-66.

[73] Pike D, Lindenmaier TJ, Sin DD, Parraga G. Imaging evidence of the relationship between atherosclerosis and chronic obstructive pulmonary disease. Imaging in Medicine 2014;6(1):53-73.

[74] Gevenois PA, De Vuyst P, De Maertelaer V, et al. Comparison of computed density and microscopic morphometry in pulmonary emphysema. American journal of respiratory and critical care medicine 1996;154(1):187-92.

[75] Washko GR, Parraga G, Coxson HO. Quantitative pulmonary imaging using computed tomography and magnetic resonance imaging. Respirology 2012;17(3):432-44.

[76] Lutey BA, Conradi SH, Atkinson JJ, et al. Accurate measurement of small airways on low-dose thoracic CT scans in smokers. CHEST Journal 2013;143(5):1321-9.

[77] Simon BA, Kaczka DW, Bankier AA, Parraga G. What can computed tomography and magnetic resonance imaging tell us about ventilation? Journal of Applied Physiology 2012;113(4):647-57.

[78] Ebert M, Grossmann T, Heil W, et al. Nuclear magnetic resonance imaging with hyperpolarised helium-3. The Lancet 1996;347(9011):1297-9.

[79] Parraga G, Mathew L, Etemad-Rezai R, McCormack DG, Santyr GE. Hyperpolarized 3 He magnetic resonance imaging of ventilation defects in healthy elderly volunteers: initial findings at 3.0 Tesla. Academic radiology 2008;15(6):776-85.

[80] Mathew L, Evans A, Ouriadov A, et al. Hyperpolarized 3 He magnetic resonance imaging of chronic obstructive pulmonary disease: reproducibility at 3.0 Tesla. Academic radiology 2008;15(10):1298-311.

[81] Fain S, Schiebler ML, McCormack DG, Parraga G. Imaging of lung function using hyperpolarized helium-3 magnetic resonance imaging: review of current and emerging translational methods and applications. Journal of Magnetic Resonance Imaging 2010;32(6):1398-408.

[82] Yablonskiy DA, Sukstanskii AL, Woods JC, et al. Quantification of lung microstructure with hyperpolarized 3He diffusion MRI. Journal of Applied Physiology 2009;107(4):1258-65.

[83] Saam BT, Yablonskiy DA, Kodibagkar VD, et al. MR imaging of diffusion of 3He gas in healthy and diseased lungs. Magnetic resonance in medicine 2000;44(2):174-9.

[84] Widmaier E, Raff H, Strang K. Vander's Human Physiology. McGraw-Hill Companies,Incorporated.

[85] Mallat ENMJ. Human Anatomy. Benjamin Cummings 2003.

[86] Caro CG. The Mechanics of the Circulation. Cambridge University Press, 2012.

[87] Kessler R, Faller M, Fourgaut G, Mennecier B, Weitzenblum E. Predictive factors of hospitalization for acute exacerbation in a series of 64 patients with chronic obstructive pulmonary disease. American journal of respiratory and critical care medicine 1999;159(1):158-64.

[88] McGhan R, Radcliff T, Fish R, Sutherland ER, Welsh C, Make B. Predictors of rehospitalization and death after a severe exacerbation of COPD. CHEST Journal 2007;132(6):1748-55.

[89] Terzano C, Conti V, Di Stefano F, et al. Comorbidity, hospitalization, and mortality in COPD: results from a longitudinal study. Lung 2010;188(4):321-9.

[90] Mohrman DE, Heller LJ. Cardiovascular Physiology. McGraw-Hill, Health Professions Division, 1997.

[91] Roeleveld RJ, Marcus JT, Boonstra A, et al. A comparison of noninvasive MRI-based methods of estimating pulmonary artery pressure in pulmonary hypertension. Journal of Magnetic Resonance Imaging 2005;22(1):67-72.

[92] Arcasoy SM, Christie JD, Ferrari VA, et al. Echocardiographic assessment of pulmonary hypertension in patients with advanced lung disease. American journal of respiratory and critical care medicine 2003;167(5):735-40.

[93] Homma A, Anzueto A, Peters JI, et al. Pulmonary artery systolic pressures estimated by echocardiogram vs cardiac catheterization in patients awaiting lung transplantation. The Journal of heart and lung transplantation 2001;20(8):833-9.

[94] Chan K-L, Currie PJ, Seward JB, Hagler DJ, Mair DD, Tajik AJ. Comparison of three Doppler ultrasound methods in the prediction of pulmonary artery pressure. Journal of the American College of Cardiology 1987;9(3):549-54.

[95] Chang C. The normal roentgenographic measurement of the right descending pulmonary artery in 1,085 cases. The American journal of roentgenology, radium therapy, and nuclear medicine 1962;87:929.

[96] Teichmann V, Ježek V, Herles F. Relevance of width of right descending branch of pulmonary artery as a radiological sign of pulmonary hypertension. Thorax 1970;25(1):91-6.

[97] Lupi E, Dumont C, Tejada V, Horwitz S, Galland F. A radiologic index of pulmonary arterial hypertension. CHEST Journal 1975;68(1):28-31.

[98] Kanemoto N, Furuya H, Etoh T, Sasamoto H, Matsuyama S. Chest roentgenograms in primary pulmonary hypertension. CHEST Journal 1979;76(1):45-9.

[99] Kuriyama K, Gamsu G, Stern RG, Cann CE, Herfkens RJ, Brundage BH. CT-determined pulmonary artery diameters in predicting pulmonary hypertension. Investigative radiology 1984;19(1):16-22.

[100] Schwedel JB, Escher DW, Aaron RS, Young D. The roentgenologic diagnosis of pulmonary hypertension in mitral stenosis. American heart journal 1957;53(2):163-70.

[101] Chan AL, Juarez MM, Shelton DK, et al. Novel computed tomographic chest metrics to detect pulmonary hypertension. BMC medical imaging 2011;11(1):7.

[102] Burger IA, Husmann L, Herzog BA, et al. Main pulmonary artery diameter from attenuation correction CT scans in cardiac SPECT accurately predicts pulmonary hypertension. Journal of Nuclear Cardiology 2011;18(4):634-41.

[103] Edwards P, Bull R, Coulden R. CT measurement of main pulmonary artery diameter. The British journal of radiology 1998;71(850):1018-20.

[104] Tan RT, Kuzo R, Goodman LR, Siegel R, Haasler GB, Presberg KW. Utility of CT scan evaluation for predicting pulmonary hypertension in patients with parenchymal lung disease. CHEST Journal 1998;113(5):1250-6.

[105] Ackman Haimovici JB, Trotman-Dickenson B, Halpern EF, et al. Relationship between pulmonary artery diameter at computed tomography and pulmonary artery pressures at right-sided heart catheterization. Academic radiology 1997;4(5):327-34.

[106] Frank H, Globits S, Glogar D, Neuhold A, Kneussl M, Mlczoch J. Detection and quantification of pulmonary artery hypertension with MR imaging: results in 23 patients. AJR American journal of roentgenology 1993;161(1):27-31.

[107] Saba T, Foster J, Cockburn M, Cowan M, Peacock A. Ventricular mass index using magnetic resonance imaging accurately estimates pulmonary artery pressure. European Respiratory Journal 2002;20(6):1519-24.

[108] Tardivon AA, Mousseaux E, Brenot F, et al. Quantification of hemodynamics in primary pulmonary hypertension with magnetic resonance imaging. American journal of respiratory and critical care medicine 1994;150(4):1075-80.

[109] Wacker CM, Schad LR, Gehling U, et al. The pulmonary artery acceleration time determined with the MR-RACE-technique: comparison to pulmonary artery mean pressure in 12 patients. Magnetic resonance imaging 1994;12(1):25-31.

[110] Marcus JT, Noordegraaf AV, Roeleveld RJ, et al. Impaired left ventricular filling due to right ventricular pressure overload in primary pulmonary hypertension: noninvasive monitoring using MRI. CHEST Journal 2001;119(6):1761-5.

CHAPTER 2: THREE-DIMENSIONAL SEGMENTATION OF PULMONARY ARTERY VOLUME FROM THORACIC COMPUTED TOMOGRAPHY IMAGING

This chapter describes the development of a three-dimensional volumetric measurement for evaluating the size of the main, left and right pulmonary arteries as well as calculating total pulmonary artery volume. The reproducibility of the volumetric measurements is also reported in this chapter.

The contents presented here has been adapted from work previously published in the SPIE Medical Imaging Conference Proceedings, Orlando, Florida, United States 2015, and is reproduced here with permission provided in Appendix B.
TJ Lindenmaier, K Sheikh, E Bluemke, I Gyacskov, M Mura, C Licskai, L Mielniczuk, A Fenster, IA Cunningham and G Parraga, Three-Dimensional Segmentation of Pulmonary Artery Volume from Thoracic Computed Tomography Imaging. SPIE Medical Imaging, Renaissance Orlando at SeaWorld, Orlando, Florida, United States, February 21-26, 2015

2.1 Introduction

Chronic obstructive pulmonary disease (COPD) affects the airways and the lung parenchyma.[1] It is currently the fourth leading cause of death in the United States and is predicted to be the third leading cause of death worldwide by 2020.[2] COPD is a heterogeneous disease with various clinical phenotypes, including chronic bronchitis, emphysema, asthma with fixed airflow obstruction, frequent exacerbation phenotype, and COPD associated with pulmonary hypertension. There is an expanding body of literature seeking to define COPD phenotypes and identify predictive biomarkers. The diagnosis of COPD is confirmed using spirometry measurements of the forced expiratory volume in one second (FEV_1) and forced vital capacity (FVC). While spirometry is a diagnostic prerequisite, it is insensitive to subclinical changes in lung function, correlates poorly with clinical symptoms including cardiovascular disease, is a poor predictor of mortality and does not accurately predict exacerbation frequency.[3, 4] In addition to airflow limitation, COPD is also associated with cardiovascular disease and abnormalities of the pulmonary vasculature. For example, COPD patients commonly develop pulmonary hypertension (PH) leading to increased morbidity and mortality.[5] Previous work has shown that PH is associated with acute exacerbations of COPD and sudden worsening of symptoms resulting in hospitalization.[6, 7] Patients with COPD frequently develop other cardiovascular abnormalities such as carotid atherosclerosis[8-13], coronary artery calcification[14-17] and

vascular dysfunction.[7, 18-20] These findings cannot be explained by smoking history alone, further emphasizing the need for new biomarkers that can predict disease development and severity.

Recent results from the Evaluation of COPD Longitudinally to Identify Predictive Surrogate Endpoints (ECLIPSE) study[21] suggested that a history of acute exacerbations of COPD was the single best predictor of future events. This finding strengthens the need for biomarkers that can predict subclinical changes in lung function, disease development and severity. Previous studies quantified the size of the pulmonary artery (PA) in order to evaluate pulmonary vasculature abnormalities as a potential predictor of COPD exacerbations. Typically, the aorta (A) and pulmonary artery (PA) are quantified using manual diameter measurements at the level of the PA bifurcation in thoracic computed tomography (CT) images.[7] It was recently shown in the COPDGene cohort (N=3464) that a PA/A ratio >1 was associated with acute exacerbations and the risk of future exacerbations.[7] Moreover, a different study showed that an increase in PA diameter was associated with subclinical PH.[22] Both of these studies utilized manual one-dimensional measurements of the pulmonary artery. To enhance sensitivity and improve observer variability, we aimed to develop a three-dimensional (3D) measurement of the PA from thoracic CT. We hypothesized that 3D volumetric measurements would have an intra-observer variability <10% and high inter-observer agreement ICC > 0.90. The 3D method is more time consuming and laborious and validation is required before a more automated approach is considered. Therefore, our objective was to develop and test the reproducibility of 3D manual volumetric PA measurement from thoracic CT images.

2.2 Methods

2.2.1 Study Subjects

All subjects provided written informed consent to a protocol that was approved by the local research ethics board (#15930) and Health Canada. A total of 15 ex-smokers aged 56-79 (mean age: 67 ± 7 years) with a smoking history > 10 pack-years were randomly chosen from a cohort of 199 subjects. Three subjects were randomly selected from each of the following four groups based on COPD disease severity using the Global Initiative for Chronic Obstructive Lung Disease (GOLD) classification: GOLD IV (FEV_1 $<30\%$), GOLD III (FEV_1 30-49%), GOLD II (FEV_1 50-79%), GOLD I ($FEV_1 \geq 80\%$) and a fifth group without airflow limitation ($FEV_1/FVC \geq 0.70$).

2.2.2 Imaging

CT images were acquired on a 64-slice Lightspeed VCT scanner (General Electric Health Care, Milwaukee, WI USA) (64×0.625mm collimation, 120 kVp, 100 effective mA, tube rotation time $= 500$ms, pitch=1.0).[23] Subjects were first coached through normal breathing. Once at functional residual capacity (FRC), subjects were instructed to inhale 1L of medical grade nitrogen gas (N_2) from a Tedlar® bag (Jansen Inert Products, Coral Springs, FL, USA)[23] to match lung volumes acquired using MRI. Imaging was performed using a spiral acquisition and reconstructed using a standard convolution kernel to 1.25mm.[23] The effective dose for an average adult was estimated at 1.8mSv using the ImPACT CT patient dosimetry calculator based on the Health Protection Agency (UK) NRPB-SR250.[24]

2.2.3   PA Segmentation: Development and Application

Reconstructed CT images were evaluated in Digital Imaging and Communications in Medicine (DICOM) format using custom-built software (3D Quantify V4.1.1, Robarts Research Institute, London, Canada) previously developed for carotid ultrasound measurements.[25] The algorithm pipeline is summarized in Figure 2-1.
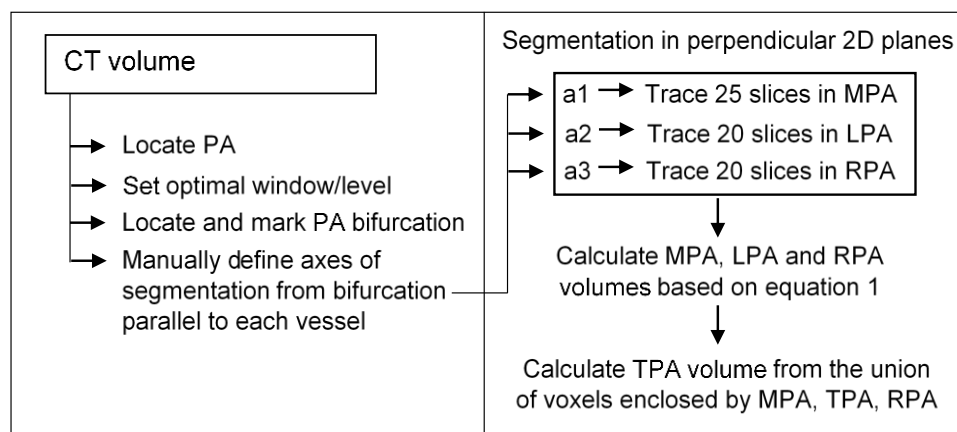
Figure 2-1: PA Volume measurement algorithm pipeline.

After setting the optimal window and level, such that the PA was well distinguished from the surrounding tissue, the observer navigated the CT volume, shown in the top left of Figure 2-2, to the plane where the bifurcation of the main pulmonary artery (MPA) into the left and right pulmonary arteries (LPA and RPA respectively) was clear, as shown in the middle left panel of Figure 2-2.
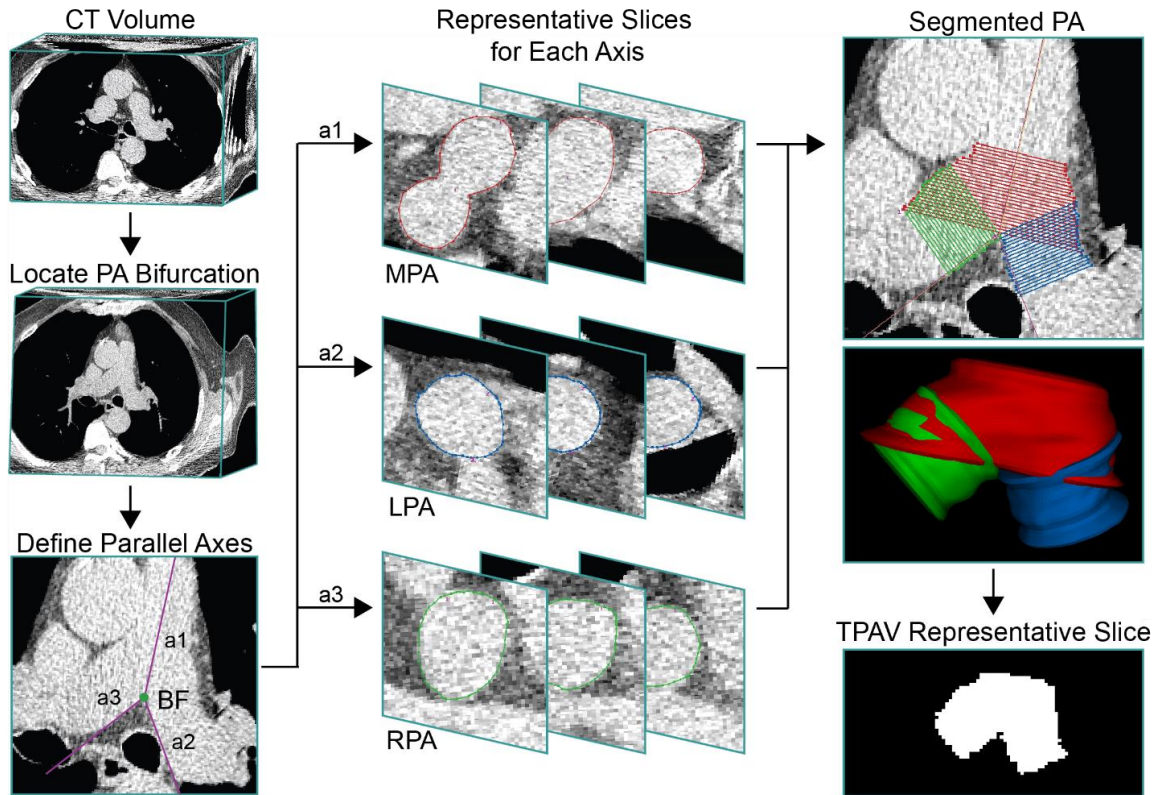
Figure 2-2: User input for PA measurement. The user first adjusted the window and level such that the PA was well distinguished from surroundings. The arterial bifurcation (BF) was identified and used as a landmark for manual placement of axes a1, a2, a3 from the BF that were parallel to the MPA, LPA and RPA respectively. The cross sectional areas in planes perpendicular to each axis of segmentation were manually traced in 25 slices for MPA and 20 slices for LPA and RPA (only 3 representative slices shown here) with inter-slice distance of 1.00 mm. The resulting volume was generated as shown in Equation 4. Voxels enclosed by each polygonal surface were extracted and their union was taken to account for the overlap between segmented vessels. The number of resulting voxels were then multiplied by the voxel dimensions to calculate TPAV. Bottom right panel shows a representative slice for the union of extracted voxels.

The user then set the bifurcation point (BF), and manually identified the first axis (a1) of segmentation from the BF parallel to the MPA. The cross-sectional area of the vessel was then manually segmented in 25 consecutive two-dimensional planes perpendicular to the axis of segmentation, starting at the BF, with an inter-slice distance (ISD) of 1.00 mm. This approach was repeated for the LPA and RPA (axes of segmentation a2 and a3 respectively) for 20 consecutive perpendicular planes, starting from the BF. Once the

vessels were traced, sub-volumes were generated by multiplying each area by half the ISD on either side of the segmented region, as shown in Figure 2-3, represented by dashed lines.
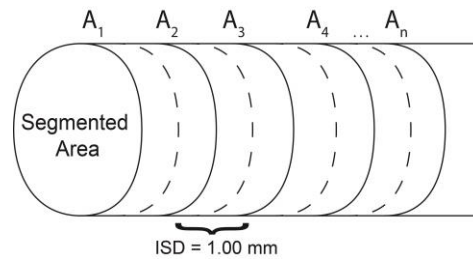
Figure 2-3: PA volume generation. Sub-volumes were generated by multiplying the area of segmented contours by half the inter-slice distance (ISD) on either side of the contour, represented by dashed lines above. To generate volume measurements, sub-volumes were summed as shown in Equation 4.

$$V = \frac{1}{2}(A_1 + A_n) + \sum_{i=2}^{n-1} A_i \tag{4}$$

The general equation for calculating volumes in millimeters cubed is expressed as shown in Equation 4. Volumes of the MPA, LPA and RPA were also obtained from generated polygonal surfaces in order to calculate a total PA volume (TPAV) for the pulmonary artery. Polygonal surfaces were generated as previously described[26] for segmentation of the carotid artery. To generate TPAV, the union of voxels enclosed by each of the MPA, LPA and RPA was taken and multiplied by the voxel dimensions. Taking the union of voxels, accounted for the overlap between polygonal surfaces. Segmentation was performed by three observers. Observer 1 (TJL) was a well-trained observer with previous experience in CT measurements of PA as well as carotid artery segmentation from ultrasound, while observers 2 (EB) and 3 (KS) received minimal training.

2.2.4   Evaluation and Statistical Analysis

Three observers evaluated MPA, LPA, RPA and TPA volumes for 15 ex-smokers. Measurements were repeated five times, and in random blinded fashion with 24 hr between measurements to reduce potential observer learning and bias. To evaluate the intra-observer variability, the coefficient of variation (CV) was generated (SD of five repeated, independent measurements divided by the mean) for each observer. Inter-observer agreement was also evaluated using linear regression and intraclass correlation (ICC) analysis. To test the long term reproducibility, observer 1 repeated measurements of the

same 15 subjects five times and intra-class correlation analysis was performed to assess agreement. Observer 1 also performed diameter measurements of the MPA as previously described[7] and the diameter mean over four consecutive center slices at the level of the bifurcation was used for this estimate. IBM SPSS Statistics for Windows v21 (IBM Corp, Armonk, NY, USA 2012) and GraphPad Prism for Windows, v6.02 (GraphPad Software, La Jolla, CA, USA) was used for all analyses. Results were considered significant when the probability of a type I error was less than 5% (p < .05).

2.3 Results and Discussion

2.3.1 Relationship between PA volume and PA diameter

Figure 2-4 shows the relationship for the MPA diameter and main pulmonary artery volume (MPAV) averaged from five rounds of measurements. A second order polynomial was used to estimate the relationship between the gold standard diameter measurements and PA volumes and showed a strong association (r^2=0.76) for PA diameter and volume. Thus, our technique is in high agreement with the gold standard diameter measurement. Three observers performed MPA, LPA, RPA and TPA volume measurements over five rounds of measurements, as previously mentioned, to evaluate inter- and intra-observer variability.
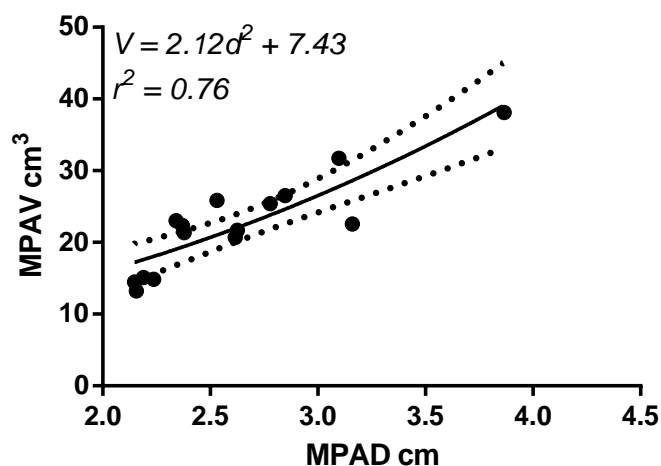
Figure 2-4: Relationship between PA volume and diameter. Second order polynomial was used to evaluate the association between novel PA volume and diameter.

2.3.2   Intra-observer variability

Figure 2-5 shows representative measurements of the same observer and different observers overlaid to visually asses the variability between measurements. Figure 2-6 shows mean CV for each subject and observer. The pooled CV for observer 1 was: MPA:2%, LPA:3%, RPA:2%, TPA:2%, for observer 2 was MPA:8%, LPA:5%, RPA:5%, TPA:6%, and for observer 3 was: MPA:3%, LPA:3%, RPA:3%, TPA:3 %.
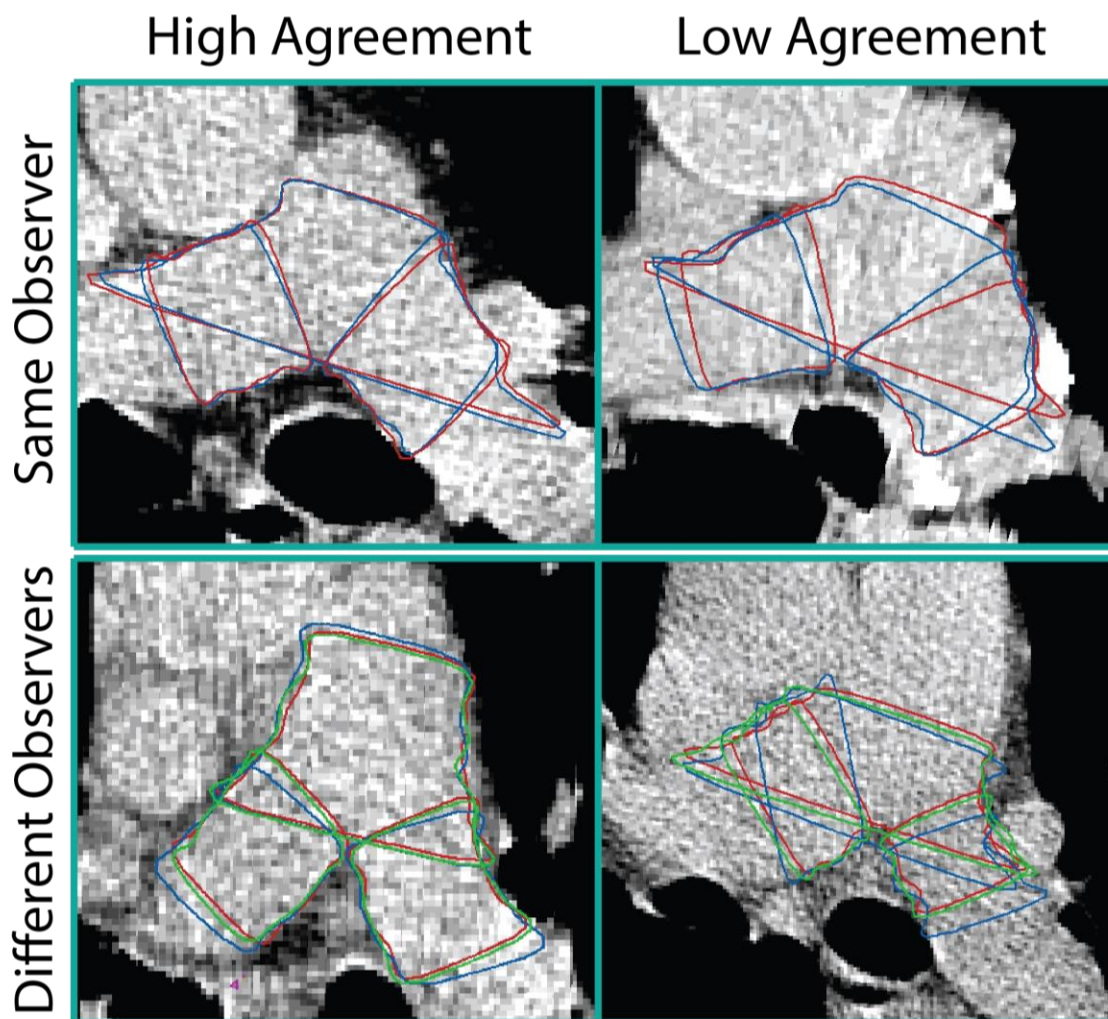
Figure 2-5: Representative measurements. Within and between observer agreements. Top panels show measurements performed by the same observer (observer 1) on two different subjects, high agreement on left and low agreement on right. Different colours represent measurements performed in two separate rounds of the trial. Bottom panels show measurements performed by three different observers (observer 1, observer 2 and observer 3), on two different subjects, with high agreement on left and low agreement on right. Red outline was performed by observer 1 (well-trained), while blue and green outlines were performed by observers 2 and 3 respectively (minimal training).
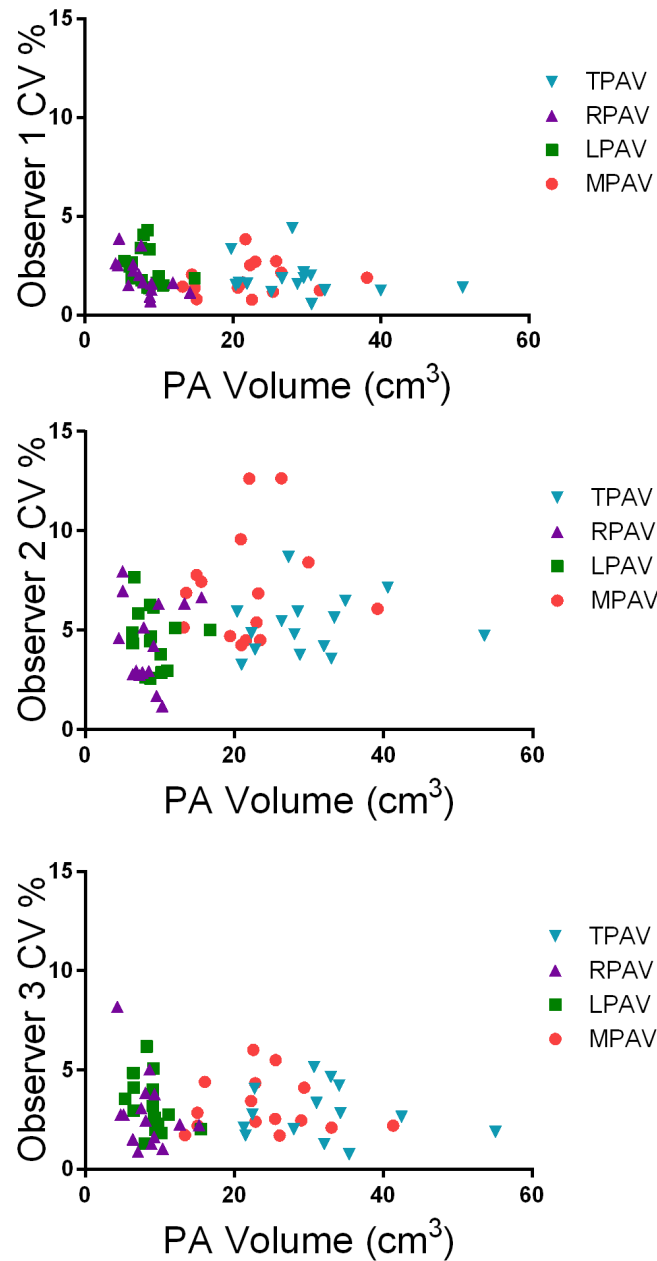
Figure 2-6: Intra-observer variability. Mean CV for Observers 1-3. ID# 178, 196 were excluded from TPA measurements for Observer 2 – Round 4 due to missing data.

2.3.3   Inter-observer variability

Figure 2-7 shows strong linear relationships for mean MPA (r^2=0.96, p<.001), LPA (r^2=0.98, p<.001) RPA (r^2=0.99, p<.001) and TPA (r^2=0.98, p<.001) volumes from the five

rounds of measurements for observers 1 and 2 as well as strong linear relationships for mean MPA (r^2=0.98, p<.001), LPA (r^2=0.98, p<.001), RPA (r^2=0.99, p<.001) and TPA (r^2=0.99, p<.001) for observers 1 and 3. ICC analysis also showed high agreement for measurements performed by three observers (ICC$_{MPA}$=0.98, ICC$_{LPA}$=0.98, ICC$_{RPA}$=0.99, ICC$_{TPA}$=0.98).
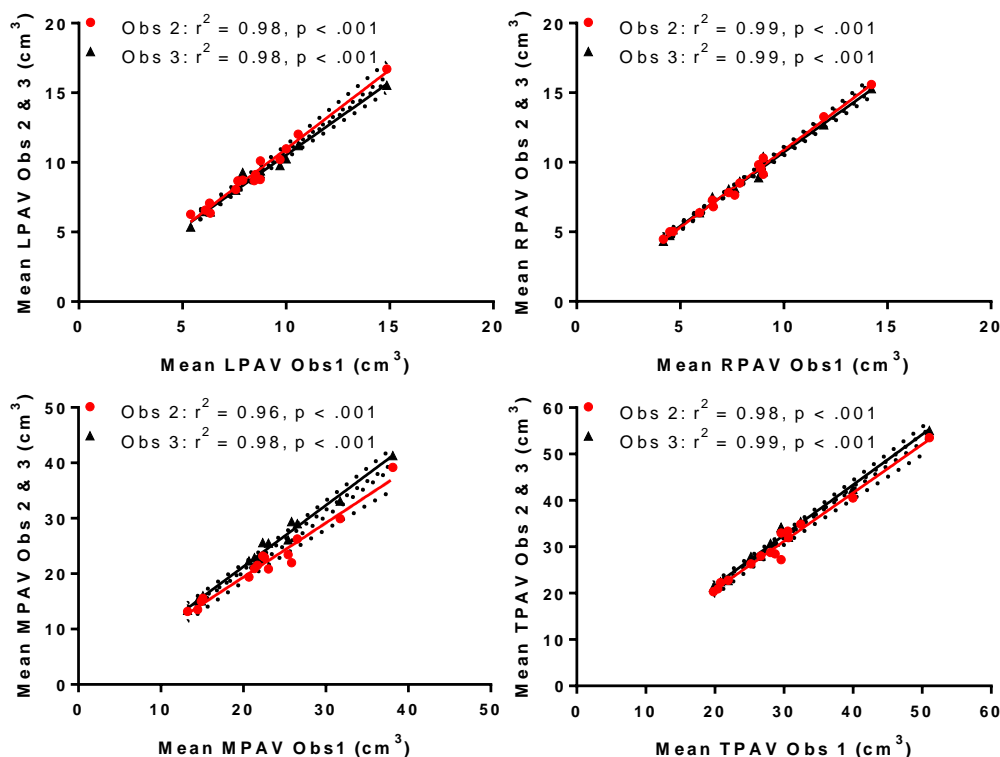
Figure 2-7: Inter-observer variability. Linear relationships for mean MPA, LPA, RPA and TPAV measurements for observer 1 (expert) with observers 2 and 3 (minimally-trained).

2.3.4   Long-term variability

To assess the long term reproducibility of our technique, observer 1 repeated five measurement rounds four months after completing the baseline reproducibility trial. ICC analysis revealed high agreement for baseline and follow-up measurements (ICC$_{MPA}$=0.998, ICC$_{LPA}$=0.995, ICC$_{RPA}$=0.998, ICC$_{TPA}$=0.997).

2.4 Conclusion

We developed a manual method to generate three-dimensional volumes at the bifurcation for the main, left and right PA. Volumetric measurements were in agreement ($r^2 = 0.76$) with PA diameter measurements, which served as the gold standard. Inter-observer variability was low with strong inter-observer correlations providing a strong rationale to automate this measurement for clinical workflows.

2.5   References

[1] Rabe KF, Hurd S, Anzueto A, et al. Global strategy for the diagnosis, management, and prevention of chronic obstructive pulmonary disease: GOLD executive summary. American journal of respiratory and critical care medicine 2007;176(6):532-55.

[2] Raherison C, Girodet P. Epidemiology of COPD. European Respiratory Review 2009;18(114):213-21.

[3] Franciosi LG, Page CP, Celli BR, et al. Markers of disease severity in chronic obstructive pulmonary disease. Pulmonary pharmacology & therapeutics 2006;19(3):189-99.

[4] Gelb AF, Hogg JC, Müller NL, et al. Contribution of emphysema and small airways in COPD. CHEST Journal 1996;109(2):353-9.

[5] Chaouat A, Naeije R, Weitzenblum E. Pulmonary hypertension in COPD. European Respiratory Journal 2008;32(5):1371-85.

[6] Kirby M, Kanhere N, Etemad-Rezai R, McCormack DG, Parraga G. Hyperpolarized helium-3 magnetic resonance imaging of chronic obstructive pulmonary disease exacerbation. Journal of Magnetic Resonance Imaging 2013;37(5):1223-7.

[7] Wells JM, Washko GR, Han MK, et al. Pulmonary arterial enlargement and acute exacerbations of COPD. New England Journal of Medicine 2012;367(10):913-21.

[8] Barr RG, Ahmed FS, Carr JJ, et al. Subclinical atherosclerosis, airflow obstruction and emphysema: the MESA Lung Study. European Respiratory Journal 2012;39(4):846-54.

[9] Engström G, Hedblad B, Valind S, Janzon L. Asymptomatic leg and carotid atherosclerosis in smokers is related to degree of ventilatory capacity: longitudinal and cross-sectional results from 'Men born in 1914', Sweden. Atherosclerosis 2001;155(1):237-43.

[10] Frantz S, Nihlén U, Dencker M, Engström G, Löfdahl CG, Wollmer P. Atherosclerotic plaques in the internal carotid artery and associations with lung function assessed by different methods. Clinical physiology and functional imaging 2012;32(2):120-5.

[11] Iwamoto H, Yokoyama A, Kitahara Y, et al. Airflow limitation in smokers is associated with subclinical atherosclerosis. American journal of respiratory and critical care medicine 2009;179(1):35-40.

[12] Lahousse L, van den Bouwhuijsen QJ, Loth DW, et al. Chronic obstructive pulmonary disease and lipid core carotid artery plaques in the elderly: the Rotterdam Study. American journal of respiratory and critical care medicine 2013;187(1):58-64.

[13] van Gestel YR, Flu W-J, van Kuijk J-P, et al. Association of COPD with carotid wall intima-media thickness in vascular surgery patients. Respiratory medicine 2010;104(5):712-6.

[14] Chae EJ, Seo JB, Oh Y-M, Lee JS, Jung Y, Do Lee S. Severity of Systemic Calcified Atherosclerosis Is Associated With Airflow Limitation and Emphysema. Journal of computer assisted tomography 2013;37(5):743-9.

[15] Dransfield MT, Huang F, Nath H, Singh SP, Bailey WC, Washko GR. CT emphysema predicts thoracic aortic calcification in smokers with and without COPD. COPD: Journal of Chronic Obstructive Pulmonary Disease 2010;7(6):404-10.

[16] McAllister DA, MacNee W, Duprez D, et al. Pulmonary function is associated with distal aortic calcium, not proximal aortic distensibility. MESA lung study. COPD: Journal of Chronic Obstructive Pulmonary Disease 2011;8(2):71-8.

[17] Rasmussen T, Køber L, Pedersen JH, et al. Relationship between chronic obstructive pulmonary disease and subclinical coronary artery disease in long-term smokers. European Heart Journal–Cardiovascular Imaging 2013;14(12):1159-66.

[18] Barr RG, Mesia-Vela S, Austin JH, et al. Impaired flow-mediated dilation is associated with low pulmonary function and emphysema in ex-smokers: the Emphysema and Cancer Action Project (EMCAP) Study. American journal of respiratory and critical care medicine 2007;176(12):1200-7.

[19] Cinarka H, Kayhan S, Gumus A, et al. Arterial stiffness measured by carotid femoral pulse wave velocity is associated with disease severity in chronic obstructive pulmonary disease. Respiratory care 2013;59(2):274-80.

[20] Sabit R, Bolton CE, Edwards PH, et al. Arterial stiffness and osteoporosis in chronic obstructive pulmonary disease. American journal of respiratory and critical care medicine 2007;175(12):1259-65.

[21] Hurst JR, Vestbo J, Anzueto A, et al. Susceptibility to exacerbation in chronic obstructive pulmonary disease. New England Journal of Medicine 2010;363(12):1128-38.

[22] Lange TJ, Dornia C, Stiefel J, et al. Increased pulmonary artery diameter on chest computed tomography can predict borderline pulmonary hypertension. Pulm Circ 2013;3(2):363-8.

[23] Kirby M, Owrangi A, Svenningsen S, et al. On the role of abnormal DLCO in ex-smokers without airflow limitation: symptoms, exercise capacity and hyperpolarised helium-3 MRI. Thorax 2013;68(8):752-9.

[24] Shrimpton P, Jones D. Normalised organ doses for x ray computed tomography calculated using Monte Carlo techniques and a mathematical anthropomorphic phantom. Radiation Protection Dosimetry 1993;49(1-3):241-3.

[25] Ainsworth CD, Blake CC, Tamayo A, Beletsky V, Fenster A, Spence JD. 3D Ultrasound Measurement of Change in Carotid Plaque Volume A Tool for Rapid Evaluation of New Therapies. Stroke; a journal of cerebral circulation 2005;36(9):1904-9.

[26] Chiu B, Egger M, Spence JD, Parraga G, Fenster A. Quantification of carotid vessel atherosclerosis. In: International Society for Optics and Photonics, 2006: 61430B-B

CHAPTER 3: PULMONARY ARTERY ABNORMALITIES IN EX-SMOKERS WITH AND WITHOUT AIRFLOW LIMITATION

This chapter describes the relationship between pulmonary artery volume measurements, described in Chapter 2, and measurements of lung function and structure in a group of COPD ex-smokers and a small group of never-smokers.

The contents of this chapter are to be submitted to the Journal of Chronic Obstructive Pulmonary Disease for peer review, April 2015.

Tamas J *Lindenmaier, Miranda Kirby, Gregory Paulin, Marco Mura, Christopher Licskai, Harvey O Coxson, Ian A Cunningham and Grace Parraga, Pulmonary Artery Abnormalities in Ex-smokers with and without Airflow Limitation, J COPD.*

3.1 Introduction

Chronic obstructive pulmonary disease (COPD) is the fourth leading cause of death in the United States and estimates predict that in 2020, COPD will be the third leading cause of death worldwide.[1] In COPD patients, chronic lung inflammation and tissue destruction is the result of long-term inhalation of toxins, mainly tobacco smoke[2], leading to the accelerated loss of lung function[3], reduced quality-of-life, and premature death.[4] As the disease progresses, those with moderate-to-severe disease are likely to experience acute events known as exacerbations.[5] These individuals experience a reduced quality of life and seek immediate medical attention which often results in hospitalization, placing a large burden on the healthcare system.

Although the hallmark feature of COPD is pulmonary airflow limitation measured using spirometry, COPD is also associated with vascular abnormalities including coronary vascular and cerebrovascular disease[6-9] and pulmonary artery abnormalities.[3] Importantly, vascular disease is the single largest cause of hospitalization in COPD patients with mild or moderate disease and after lung cancer, the leading cause of death.[10, 11] There is also a dose-response relationship for pulmonary structure-function abnormalities with carotid atherosclerosis[12-17], coronary artery calcification[6-9] and vascular dysfunction.[3, 18-20] While this previous work showed the importance of vascular disease in COPD patients that cannot be explained by smoking history alone[12, 13, 15-17, 21], the mechanisms of vascular disease acceleration in COPD patients are not well-established.

We recently showed that ex-smokers with normal airflow measurements reported significantly greater ventilation abnormalities, measured using hyperpolarized noble gas magnetic resonance imaging (MRI), and more severe carotid atherosclerosis as compared to never-smokers.[22] This study exploited the sensitivity of three-dimensional (3D) pulmonary MRI and carotid ultrasound and provided quantitative evidence of mild airways disease and carotid plaque that was significantly greater in ex-smokers as compared to never-smokers. Based on these previous findings, we sought to ascertain whether there were also pulmonary artery abnormalities in otherwise normal ex-smokers without airflow limitation. This is important because there is a dearth of direct evidence relating subclinical pulmonary disease (airways disease and emphysema) with pulmonary artery abnormalities in otherwise healthy ex-smokers. We aimed therefore to quantify any potential underlying relationships between pulmonary airway and parenchymal abnormalities with pulmonary artery abnormalities in mild and subclinical COPD. We also aimed to quantitatively compare pulmonary artery morphology in normal ex- and healthy never-smokers as well as in COPD patients. The relationship of pulmonary artery abnormalities[3] and pulmonary hypertension[23-25] with lung abnormalities in COPD is well-established. In one recent example, the relationship of pulmonary artery abnormalities with acute exacerbations of COPD[3] was shown, but the relevance of this for clinical practice was not ascertained. This was an important results because until now there are very few quantitative biomarkers available that help predict COPD exacerbations.[3, 26]

Here our objective was to measure three-dimensional pulmonary artery vessel measurements from thoracic CT as well as pulmonary airways disease and emphysema measurements from thoracic CT and MRI in a small group of ex-smokers and a control group of healthy never-smokers. In the subset of patients with COPD and based on previous findings that related 1D pulmonary artery measurements and exacerbations in the large-scale ECLIPSE and COPDgene cohorts, we also aimed to determine the sensitivity of 3D pulmonary artery measurements to COPD exacerbations. We hypothesized that quantitative 3D imaging measurements of the pulmonary artery, airways and parenchyma would reveal the direct relationships of early or subclinical pulmonary disease with pulmonary artery abnormalities in ex-smokers.

3.2   Methods

3.2.1   Study Participants

All research volunteers provided written informed consent to a protocol, approved by a local research ethics board and Health Canada. We conducted retrospective analysis of a group of ex-smokers with or without airflow limitation and healthy never-smoker subjects which served as the control group. The inclusion criteria for COPD ex-smokers included smoking history $\geq$10 pack-years, 50-85 years of age with a physician diagnosis of COPD and post-bronchodilator forced expiratory volume in 1 second (FEV_1)/forced vital capacity (FVC) ratio <0.70, in accordance with the Global initiative for chronic Obstructive Lung Disease (GOLD) criteria.[27] Ex-smokers without airflow limitation were enrolled with the same age-range and smoking history but with FEV_1/FVC $\geq$0.70. Exclusion criteria included a current diagnosis of asthma or other respiratory conditions. We did not prospectively exclude subjects with other COPD co-morbidities. The inclusion criteria for the healthy never-smokers was 60 to 90 years of age with a smoking history of <0.5 pack-years and no history of unstable cardiovascular disease or chronic respiratory disease.

Because of the significant impact of exacerbations on COPD patient mortality[28], we recorded severe exacerbations requiring hospitalization for all patients with COPD. The number of acute exacerbations requiring hospitalization was determined using patient hospital records (PowerChart® Cerner Corporation, Missouri, USA) as previously described.[29] The total number of hospitalizations was defined as the total number of hospitalizations that occurred between 2.5yr prior to and 2.5yr following the study visit (from time -2.5 to 2.5 years). The number of prior hospitalizations was defined as the total number of hospitalizations between 2.5yr and 5yr prior to the study visit (from time -5 to -2.5 years).

3.2.2   Spirometry, plethysmography, quality of life and exercise capacity measurements

Spirometry and lung volumes were acquired using body plethysmography (MedGraphics Corporation, St Paul, Minnesota, USA) following American Thoracic Society and European Respiratory Society (ERS) guidelines;[30] the attached gas analyzer

(MedGraphics) was used to measure the diffusing capacity for carbon monoxide (DL_{CO}). Quality of life was assessed using the St. George's Respiratory Questionnaire (SGRQ)[31, 32]; exercise capacity was measured using a standard 6-Minute Walk Distance Test (6MWD)[33].

3.2.3   Image acquisition

MRI was performed using a 3.0 Tesla MR750 (General Electric Health Care, Milwaukee, WI) system[34] for acquisition of conventional ^{1}H, ^{3}He static ventilation and ^{3}He diffusion-weighted MRI. Conventional ^{1}H MRI was acquired during 1.0L breath-hold of N_2 from a 1.0 L Tedlar® bag from functional residual capacity (FRC). Prior to ^{3}He static ventilation and ^{3}He diffusion-weighted MRI, a spin-exchange polarizer system (Polarean, Durham, NC, USA) was used to polarize ^{3}He gas to 30-40%. ^{3}He static ventilation and diffusion-weighted imaging were performed following inhalation of a ^{3}He/N_2 gas mixture (^{3}He dose = 5 ml/kg body weight) from a 1.0 L Tedlar® bag from FRC as previously described.[34]

Multi-detector CT was performed using the 64-slice Lightspeed VCT system (GEHC, Milwaukee, WI USA) with participants in breath-hold after inhalation of 1.0L of N_2 from FRC[35] in order to match the MRI lung volume. The ECLIPSE imaging protocol[36] was adapted and used: 64x0.625mm collimation, 120kVp, 100 effective mA, 500ms tube rotation time, pitch of 1.00 and image reconstruction using a standard convolution kernel to 1.25mm. We calculated radiation dose according to our manufacturer settings using the ImPACT CT patient dosimetry calculator based on the Health Protection Agency (UK) NRPB-SR250 and the total effective dose for an average adult was 1.8 mSv.[37]

3.2.4   Image analysis

All MRI and CT analyses were performed by an expert in quantitative imaging analysis (M.K) with five years of experience developing and performing semi-automated ^{3}He MRI segmentation using custom-built software generated using MATLAB R2007b (The Math-works Inc., Massachusetts, USA). The inter- and intra-reproducibility of the ^{3}He MRI segmentation software was previously evaluated in subjects with COPD[38] and therefore MR images were evaluated once by a single expert observer. ^{3}He MRI ventilation defect percent (VDP) was quantified by registering the ^{3}He static ventilation images to the ^{1}H MR

images in order to delineate the defect boundary as previously described.[39] [3]He apparent diffusion coefficient (ADC) maps were also generated from [3]He diffusion-weighted images as previously described.[40]

Pulmonary CT measurements were generated using Pulmonary Workstation 2.0 (VIDA Diagnostics, Inc., Coralville, IA) including airway wall area (WA) and lumen area (LA) for 5th generation airways[41], the relative area of the CT density histogram with attenuation values < -950 HU (RA_{950})[42], and low attenuation clusters (LAC) of connected regions with CT densitometry values < -950 HU.[43]

For volumetric analysis of the pulmonary arteries, DICOM (Digital Imaging and Communications in Medicine) thoracic CT images were evaluated using custom-built software (3D Quantify V4.1.1, Robarts Research Institute, London, Canada), originally developed for three-dimensional visualization and quantification of carotid ultrasound volumes.[44] The main pulmonary artery volume, left pulmonary artery volume and right pulmonary artery volume were generated, as previously described.[45] As shown in Figure 3-1, the bifurcation of the main pulmonary artery was identified as the branch-point between the left and right pulmonary arteries. As previously described[45], the axes of segmentation were established from the bifurcation (BF) parallel to each of the main, left and right pulmonary arteries. The artery wall boundary was manually segmented in planes perpendicular to the axes of segmentation for 25 x 1mm slices for the main and 20 x 1mm slices for the left and right pulmonary arteries. Based on the segmented areas and the inter-slice distance, a volume for the segmented region of the vessel was generated. Total pulmonary artery volume was also generated as previously described.[45] To account for overlapping regions between main, left and right pulmonary artery volume measurements, the union of voxels enclosed by each boundary was taken and multiplied by the voxel dimensions. We previously reported low inter- and intra-observer variability for pulmonary artery volumetric measurements and therefore measurements were performed by a single observer (T.J.L.).[45] To account for gender differences in pulmonary artery volumes, measurements were normalized by body surface area and age.

It was previously shown that the pulmonary artery to aorta diameter ratio was associated with a history of COPD exacerbations and future exacerbations.[3] Therefore, we measured the main pulmonary artery and aorta diameters as previously described[3], averaged from four consecutive centre CT slices where the bifurcation was visible.
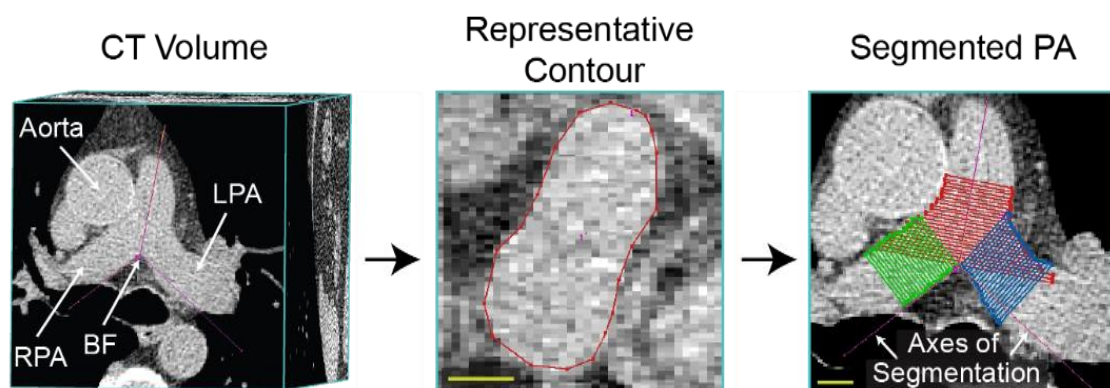
Figure 3-1: PA volume measurements methodology. Left panel depicts CT volume and the level of the bifurcation (BF) where the axes of segmentation are defined from the BF parallel to each of the MPA, LPA and RPA. The middle panel outlines a representative slice of the segmented artery. In the right panel the segmented MPA, LPA and RPA are shown.

3.2.5   Statistical Analysis

We used IBM SPSS Statistics for Windows v21 (IBM Corp, Armonk, NY, USA 2012) and GraphPad Prism for Windows, v6.02 (GraphPad Software, La Jolla, CA, USA) for statistical analyses. A one-way analysis of variance (ANOVA) with post-hoc Tukey HSD (Honest Significant Differences) was conducted to evaluate differences between groups. Pearson correlations were determined for pulmonary artery volumes and pulmonary function measurements. We also performed univariate correlations for the total number of severe exacerbations with all clinical, physiological and imaging measurements. A multivariate zero-inflated Poisson model was used to evaluate the relationship between the total number of severe exacerbations with physiological and imaging measurements using the PROC COUNTREG procedure in SAS 9.2 software (SAS Institute, Cary, NC). All measurements with significant univariate correlations were included in the multivariate

model. A zero-inflated Poisson model[46] was used because the total number of hospitalizations included a large proportion of zeroes. From the significant multivariate model, we reported the fold-change in total exacerbations which was defined as the regression coefficient divided by the standard error. Cox regressions were conducted to determine hazard ratios for the occurrence of first exacerbation post visit. Results were considered significant when the probability of a type I error was less than 5% ($p < .05$).

3.3 Results

3.3.1 Subject Characteristics

Table 3-1 shows the demographic characteristics for the study population which was a convenience sample of 35 never-smokers (71±7y) and 124 ex-smokers including 68 ex-smokers with airflow limitation (71± 9y) and 56 ex-smokers without airflow limitation (69 ±10y). One-way analysis of variance (ANOVA) showed significant differences between the three subgroups for most parameters but not for age (p=.3) or 6MWD (p=.06). For the two ex-smoker subgroups, there were significant differences for $FEV_1\%_{pred}$ (p<.001), FEV_1/FVC (p<.001), $FRC\%_{pred}$ (p<.001), $TLC\%_{pred}$ (p<.001), $DL_{CO}\%_{pred}$ (p<.001), VDP (p<.001), ADC (p<.001), RA_{950} (p<.001), airway count (p<.001), and the main (p=.014), right (p=.001) and total (p=.003) pulmonary artery volume.

Table 3-1 Subject Characteristics

	Never-Smokers (n=35) Mean (±SD)	FEV$_1$/FVC ≥ 70% (n=56) Mean (±SD)	FEV$_1$/FVC < 70% (n=68) Mean (±SD)	Sig. Diff. p
Age yrs	71 (7)	69 (10)	71 (9)	.29
BMI kg/m^2	26 (3)	29 (4)	27 (4)	**<.001**
Pack years	-	28 (17)	47 (29)	**<.001**
FEV$_1$ %$_{pred}$	107 (18)	98 (17)	63 (23)	**<.001**
FEV$_1$/FVC %	77 (6)	80 (6)	50 (13)	**<.001**
FRC %$_{pred}$	104 (22)	95 (19)	139 (36)	**<.001**
TLC %$_{pred}$	100 (14)	101 (12)	118 (18)	**<.001**
DL$_{CO}$ %$_{pred}$	91 (16)	79 (20)	54 (19)	**<.001**
SGRQ	-	25 (21)	40 (17)	**<.001**
6MWD m	-	401 (96)	369 (90)	.06
^{3}He MRI VDP %	3 (2)	6 (3)	18 (10)	**<.001**
^{3}He MRI ADC cm^2/s	0.29 (0.03)	0.28 (0.04)	0.42 (0.11)	**<.001**
CT RA$_{950}$ %	1 (1)	1 (1)	11 (11)	**<.001**
WA%	67 (2)	65 (2)	65 (2)	**.001**
Airway count	132 (40)	109 (38)	78 (29)	**<.001**
Main PA Volume cm^3	21 (4)	24 (3)	25 (4)	**<.001**
Left PA Volume cm^3	8 (1)	9 (1)	10 (1)	**<.001**
Right PA Volume cm^3	8 (1)	9 (1)	10 (2)	**<.001**
Total PA Volume cm^3	28 (4)	31 (3)	33 (5)	**<.001**

BMI = Body Mass Index; FEV$_1$ = Forced Expiratory Volume in 1 Second; %pred = Percent Predicted; FVC = Forced Vital Capacity; FRC = Functional Residual Capacity; TLC = Total Lung Capacity; RV = Residual Volume; DL$_{CO}$ = Diffusing Capacity for Carbon Monoxide; 6MWD = Six Minute Walk Distance; VDP = Ventilation Defect Percent; ADC = Apparent Diffusion Coefficient; RA$_{950}$ = CT attenuation values below -950 HU; WA% = Wall Area Percent; PA = Pulmonary Artery; SD = Standard Deviation; Sig. Diff. = significant difference between ex-smokers with and without airflow limitation and never-smokers. Main, left, right and total PA volumes adjusted for body surface area and age.

3.3.2   Imaging Measurements

Figure 3-2 shows qualitative results including hyperpolarized ^{3}He MRI static ventilation images, ADC maps, CT airway trees as well as pulmonary artery segmentations for four representative subjects. Subject 1 is a 76y male ex-smoker with grade II COPD, significant emphysema and ventilation defects and visibly enlarged main, left, right and total pulmonary volume. Subject 2 is an 86y male ex-smoker with GOLD grade III COPD, significant emphysema and ventilation defects and significantly enlarged main, left, right and total pulmonary artery volume.
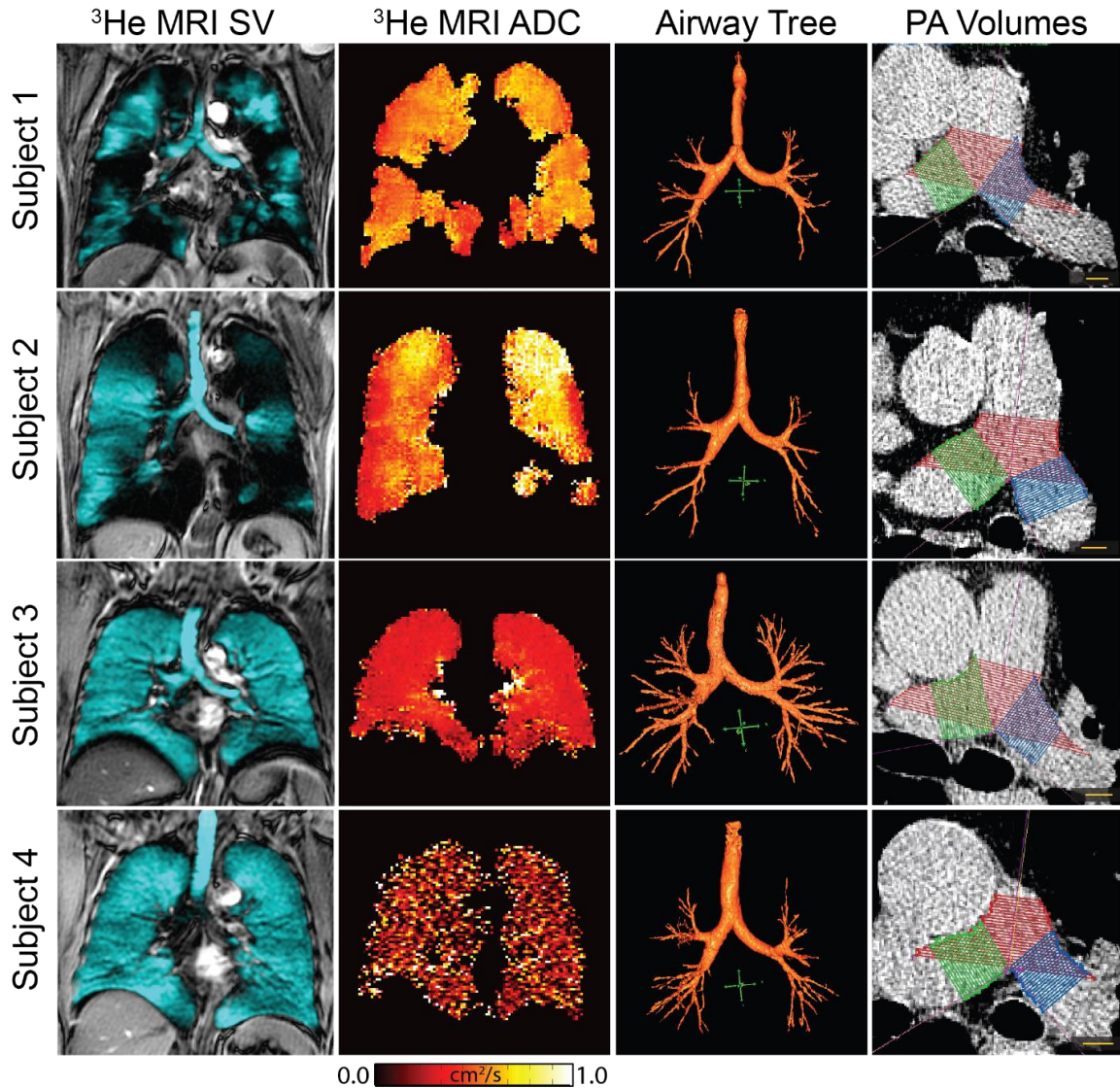
Figure 3-2: Representative subject measurements
Subject 1 is a 76y male ex-smoker with GOLD grade II COPD and FEV_1/FVC=39%, $FEV_1\%_{pred}$=56%, VDP=24%, ADC=0.50cm^2/s, WA%=66%, main pulmonary artery volume=29cm^3, left pulmonary artery volume =11cm^3, right pulmonary artery volume =11cm^3 and total pulmonary artery volume=38cm^3; Subject 2 is a 86y male ex-smoker with GOLD grade III COPD and FEV_1/FVC = 35%, $FEV_1\%_{pred}$ = 38%, VDP =30%, ADC= 0.48cm^2/s, WA% = 67%, main pulmonary artery volume =30cm^3, left pulmonary artery volume= 11cm^3, right pulmonary artery volume = 12cm^3 and total pulmonary artery volume = 40cm^3; Subject 3 is a 67y male ex-smoker FEV_1/FVC=94%, $FEV_1\%_{pred}$ =103%, VDP= 5%, ADC = 0.30cm^2/s, WA% = 56%, main pulmonary artery volume =24cm^3, left pulmonary artery volume = 9cm^3, right pulmonary artery volume =9cm^3 and total pulmonary artery volume=31cm^3; Subject 4 is a 73y male never-smoker FEV_1/FVC=76%, $FEV_1\%_{pred}$=122%, VDP= 2%, ADC = 0.34cm^2/s, WA%=66%, main pulmonary artery volume=20cm^3, left pulmonary artery volume =8cm^3, right pulmonary artery volume =8cm^3 and total pulmonary artery volume =28cm^3. Scale bars=1cm.

In contrast, Subject 3 is a 67y male ex-smoker with normal airflow measurements (FEV_1/FVC= 94%, $FEV_1\%_{pred}$=103%) and few ventilation abnormalities concomitant with mild emphysema (VDP=5%, ADC=0.30cm^2/s) and with modest main (24 cm^3), left (9cm^3), right (9cm^3) and total pulmonary artery volume (31 cm^3). Finally, subject 4 is a 73y male never-smoker with normal airflow, no ventilation abnormalities or emphysema, and visibly smaller main (20cm^3), left (8cm^3), right (8cm^3) and total pulmonary artery volume (28cm^3). Figure 3-2 shows that subjects 1 and 2 have visibly obvious ventilation defects while for subjects 3 and 4 there is homogeneous ventilation throughout the lung. In a similar fashion, ADC maps indicated greater emphysematous destruction in subjects 1 and 2 as compared to subjects 3 and 4. Furthermore, subjects 3 and 4 appear to report more complete airway trees, while subjects 1 and 2, presented with truncated airway trees that was coincident with greater pulmonary artery volumes for subjects 1 and 2 as compared to subjects 3 and 4.

Figure 3-3 and Table 3-1 show quantitative measurements and the significant differences in pulmonary artery volumes between ex- and never-smokers. As shown in Figure 3-3, there were significantly greater main, left, right and total pulmonary artery volumes in ex-smokers with and without airflow limitation as compared to never-smokers ($p<.01$). In addition, ex-smokers with airflow limitation presented with greater main, right and total pulmonary artery volumes compared to ex-smokers without airflow limitation ($p=.01$).
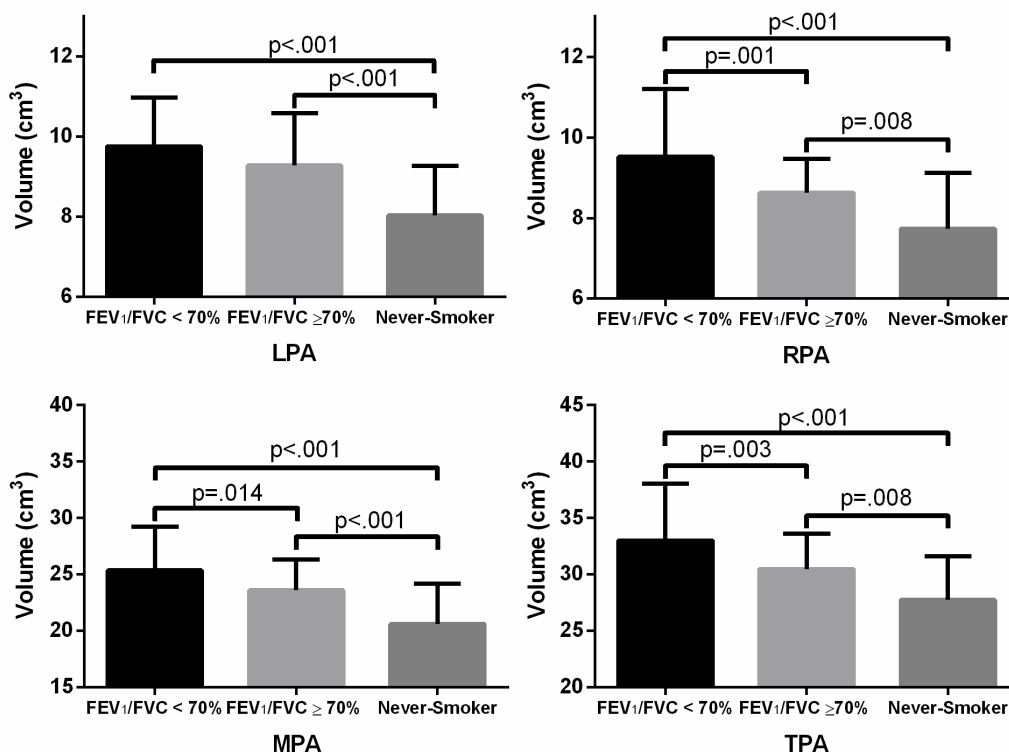
Figure 3-3: PA Volume Differences between Ex-smokers and Never-Smokers. Post-hoc analysis revealed significant differences between ex- and never- smokers for all PA volumes. Significant differences in pulmonary artery volume were also observed between ex-smokers with and without airflow limitation except for the left pulmonary artery.

3.3.3   Relationships

Table 3-2 shows Pearson Correlations for pulmonary artery volumes with measurements of emphysema, airways disease and airflow limitation for healthy never-smokers and all ex-smokers by subgroup.   For all subjects, there were significant correlations for FEV_1/FVC, $FEV_1\%_{pred,}$ $DL_{CO}\%_{pred}$, airway count, VDP and ADC with main, left, right and total pulmonary artery volume. For all ex-smokers, VDP was significantly correlated with main (r=0.23, p=.009), left (r=0.20, p=.028), right (r=0.27, p=.003) and total (r=0.25, p=.005) pulmonary artery volume and FEV_1/FVC with right pulmonary artery volume (r=-0.19, p=.03).   For ex-smokers with airflow limitation, there were no significant correlations but in ex-smokers without airflow limitation, there were significant correlations for main (r = 0.28, p = .037), right (r = 0.38, p = .004) and total (r = 0.32, p = .016) pulmonary artery volume with ADC only. For never- smokers,   there   were numerous significant correlations including for $FEV_1\%_{pred}$ with main pulmonary artery

volume

(r=-0.37, p=.03), for FEV$_1$/FVC with main (r=-0.36, p=.04), left (r=-0.40, p=.02), right (r=-0.39, p=.02) and total (r=-0.39, p=.02) pulmonary artery volume, for airway count with main pulmonary artery volume (r=-0.38, p=.026), for VDP with main (r=0.45, p=.007), left (r=.045, p=006), right (r=0.46, p=.006) and total (r=0.46, p=.006) pulmonary artery volume, and for ADC with left (r=0.35, p=.04), right (r=0.34, p=.045), and total (r=0.34, p=.047) pulmonary artery volume.

Table 3-2 Pearson correlations for pulmonary artery volumes

Parameter	MPAV r (p)	LPAV r (p)	RPAV r (p)	TPAV r (p)
All Subjects (n=159)				
FEV$_1$/FVC %	**-0.26 (<.001)**	**-0.23 (.003)**	**-0.30 (<.001)**	**-0.28 (<.001)**
FEV$_1$ %$_{pred}$	**-0.24 (.002)**	**-0.22 (.007)**	**-0.23 (.004)**	**-0.21 (.007)**
DL$_{CO}$ %$_{pred}$	**-0.22 (.006)**	**-0.21 (.009)**	**-0.26 (.001)**	**-0.24 (.002)**
Airway count	**-0.31 (<.001)**	**-0.28 (<.001)**	**-0.27 (.001)**	**-0.26 (.001)**
RA$_{950}$ %	0.14 (.08)	0.15 (.07)	**0.17 (.031)**	**0.16 (.042)**
VDP %	**0.37 (<.001)**	**0.35 (<.001)**	**0.38 (<.001)**	**0.37 (<.001)**
ADC cm^2/s	**0.21 (.008)**	**0.20 (.012)**	**0.24 (.002)**	**0.23 (.003)**
All Ex-smokers (n=124)				
FEV$_1$/FVC %	-0.14 (.12)	-0.09 (.33)	**-0.19 (.03)**	-0.17 (.06)
FEV$_1$ %$_{pred}$	-0.02 (.82)	0.003 (.97)	-0.05 (.58)	-0.04 (.69)
DL$_{CO}$ %$_{pred}$	-0.06 (.53)	-0.01 (.95)	-0.13 (.15)	-0.11 (.25)
Airway count	-0.09 (.31)	-0.08 (.37)	-0.10 (.29)	-0.09 (.30)
RA$_{950}$ %	0.03 (.73)	0.03(.77)	0.08 (.35)	0.07 (.43)
VDP %	**0.23 (.009)**	**0.20 (.028)**	**0.27 (.003)**	**0.25 (.005)**
ADC cm^2/s	0.11 (.24)	0.08(.38)	0.16 (.081)	0.14 (.12)
Ex-smokers FEV$_1$/FVC < 70% (n=68)				
FEV$_1$/FVC %	0.18 (.13)	0.18 (.15)	0.17 (.16)	0.17 (.16)
FEV$_1$ %$_{pred}$	0.23 (.05)	0.24 (.05)	0.24 (.05)	0.24 (.05)
DL$_{CO}$ %$_{pred}$	0.14 (.26)	0.11 (.36)	0.09 (.45)	0.10 (.43)
Airway count	0.08 (.50)	0.09 (.46)	0.10 (.43)	0.10 (.44)
RA$_{950}$ %	-0.16 (.20)	-0.13 (.28)	-0.12 (.34)	-0.12 (.33)
VDP %	0.09 (.47)	0.09 (.46)	0.09 (.46)	0.09 (.46)
ADC cm^2/s	-0.15 (.23)	-0.13 (.29)	-0.12 (.34)	-0.12 (.33)
Ex-smokers FEV$_1$/FVC ≥ 70% (n=56)				
FEV$_1$/FVC %	-0.07 (.59)	0.02 (.90)	-0.17 (.21)	-0.11 (.41)
FEV$_1$ %$_{pred}$	0.10 (.45)	0.07 (.60)	0.13 (.34)	0.12 (.40)
DL$_{CO}$ %$_{pred}$	0.03 (.84)	0.12 (.39)	-0.07 (.61)	-0.01 (.94)
Airway count	-0.07 (.60)	-0.09 (.53)	-0.05 (.69)	-0.07 (.63)
RA$_{950}$ %	0.23 (.09)	0.17 (.22)	0.28 (.04)	0.25 (.07)
VDP %	0.23 (.09)	0.22 (.10)	0.22 (.11)	0.23 (.10)
ADC cm^2/s	**0.28 (.037)**	0.17 (.21)	**0.38 (.004)**	**0.32 (.016)**

Never-Smokers (n=35)			
FEV$_1$/FVC %	**-0.36 (.035)**	**-0.40 (.019)**	**-0.39 (.020)**	**-0.39 (.020)**
FEV$_1$ %$_{pred}$	**-0.37 (.030)**	-0.25 (.15)	-0.27 (.12)	-0.27 (.11)
DL$_{CO}$ %$_{pred}$	0.06 (.75)	-0.05 (.80)	-0.03 (.87)	-0.03 (.89)
Airway count	**-0.38 (.026)**	-0.24 (.16)	-0.26 (.12)	-0.27 (.11)
RA$_{950}$ %	-0.12 (.49)	0.00 (.98)	-0.02 (.90)	-0.03 (.87)
VDP %	**0.45 (.007)**	**0.45 (.006)**	**0.46 (.006)**	**0.46 (.006)**
ADC cm^2/s	0.28 (.10)	**0.35 (.039)**	**0.34 (.045)**	**0.34 (.047)**

FEV1 = Forced Expiratory Volume in 1 Second; DLCO = Diffusing Capacity for Carbon Monoxide; RA950 = CT attenuation < -950 HU; VDP = Ventilation Defect Percent; ADC = Apparent Diffusion Coefficient; MPAV = Main Pulmonary Artery Volume; LPAV = Left Pulmonary Artery Volume; RPAV = Right Pulmonary Artery Volume; TPAV = Total Pulmonary Artery Volume.

In the 68 COPD ex-smokers, there were four previous exacerbations in the 2.5 year period between 5 and 2.5 years prior to the imaging visit and 46 total exacerbations in the 5 year period between 2.5 years prior to 2.5 years post visit. Table 3-3 shows the result of a multivariate model for predicting the total number of exacerbations in these 68 patients. Since there were no univariate correlations for age, body surface area, RA$_{950}$, WA%, ^{3}He MRI ADC, pulmonary artery/aorta diameter ratio, main pulmonary artery volume, and right pulmonary artery volume with total exacerbations, they were not included in the multivariate model. As shown in Table 3-3, FEV$_1$%$_{pred}$ was significantly (p=.004) associated with the total number of exacerbations with a three-fold increase in the number of total exacerbations predicted by a decrease of 1%predicted in FEV$_1$. In addition, DL$_{CO}$ was also significantly associated (p=.03) with exacerbations; a two-fold increase in total exacerbations was predicted by an increase in DL$_{CO}$ of 1%predicted. Exercise capacity (6MWD) was significantly (p=.04) associated with exacerbations; a two-fold increase in total exacerbations was related to a one meter decrease in the distance walked. Finally, total pulmonary artery volume was significantly (p=.03) associated with the total number of exacerbations; for every 1cm^3 increase in total pulmonary artery volume, a two-fold increase in total exacerbations was predicted.

Table 3-3 Relationships with total exacerbations in COPD (n=68)

Parameter (+/- SD)	Relationships With Total Exacerbations (2.5 yrs prior to 2.5 yrs post visit)		
	Univariate	Multivariate Model	
	r (p)	Fold Change	p
Age yrs	0.15 (.23)	-	-
BSA m^2	-0.07 (.58)	-	-
Previous Exacerbations (5 to 2.5 yrs prior visit)	**0.64 (<.001)**	1.75	.08
FEV$_1$ %$_{pred}$	**-0.38 (.002)**	-2.88	**.004**
DL$_{CO}$ %$_{pred}$	**-0.26 (.034)**	2.12	**.03**
RV/TLC %$_{pred}$	**0.31 (.011)**	-0.87	.38
SGRQ Score	**0.36 (.003)**	0.05	.96
6MWD m	**-0.36 (.003)**	-2.08	**.04**
CT RA$_{950}$ %	0.19 (.12)	-	-
WA%	0.10 (.42)	-	-
Airway Count	**-0.36 (.002)**	-1.26	.21
^{3}He MRI VDP %	**0.32 (.008)**	0.73	.46
^{3}He MRI ADC cm^2/s	0.14 (.25)	-	-
PA/A diameter	0.11 (.37)	-	-
Main PA Volume cm^3	0.22 (.07)	-	-
Left PA Volume cm^3	**0.33 (.005)**	-0.24	.81
Right PA Volume cm^3	0.24 (.051)	-	-
Total PA Volume cm^3	**0.25 (.037)**	2.12	**.03**

BSA = Body Surface Area; FEV$_1$ = Forced Expiratory Volume in 1 Second; DL$_{CO}$ = Diffusing Capacity for Carbon Monoxide; RV = Residual Volume; TLC = Total Lung Capacity; SGRQ = St. George's Respiratory Questionnaire; 6MWD = Six Minute Walk Distance; RA$_{950}$ = CT attenuation values below -950 HU; WA% = Wall Area Percent of 5th generation airways; VDP = Ventilation Defect Percent; ADC = Apparent Diffusion Coefficient; PA = Pulmonary Artery, A = Aorta;

3.4 Discussion

Our objective was to evaluate three-dimensional measurements of the pulmonary artery derived from thoracic CT[45] in a relatively small group of 159 never-smokers and ex-smokers with and without COPD. We observed: 1) pulmonary artery volumes were significantly greater in ex-smokers compared to never-smokers, and significantly greater in ex-smokers with airflow limitation as compared to ex-smokers with normal lung function, 2) pulmonary artery volumes were associated with pulmonary structure and function measurements when all subjects were grouped together, and, 3) a small change of

$1cm^3$ in total pulmonary artery volume predicted a 2-fold change in the number of exacerbations in 68 COPD patients.

First, we evaluated differences in pulmonary artery volumes for never-smokers and ex-smokers with and without airflow limitation. We observed significantly greater pulmonary artery volumes for ex-smokers with airflow limitation as compared to ex-smokers without airflow limitation. This is important because previous research[25] showed that pulmonary artery size is associated with pulmonary hypertension, a relatively common finding in COPD patients and concomitant with increased morbidity and mortality[25, 47] in these patients. Furthermore, we observed significantly greater pulmonary artery volumes for ex-smokers without airflow limitation as compared to never-smokers. This finding suggests that the pulmonary arteries are abnormally enlarged even in ex-smokers without obstruction. These results demonstrate that early or mild pulmonary abnormalities may be present even at early stages of the disease, which may play an important role in predicting patient outcomes.

We evaluated the relationship of the main, left, right and total pulmonary artery volume with $FEV_1\%_{pred}$, FEV_1/FVC, $DLCO\%_{pred}$, as well as CT and MRI airway and emphysema measurements. It is interesting to note that when we grouped all ex- and never-smokers together, we observed modest correlations between pulmonary artery volumes and measurements of lung function and structure. We also expected to observe these trends when analyzing ex-smokers with airflow limitation alone, as previous work demonstrated that individuals with a greater pulmonary artery to aorta diameter ratio had significantly declined lung function.[3] However, when analyzing ex-smokers with airflow limitation alone, we did not observe significant correlations between pulmonary artery volumes and lung function-structure measurements, suggesting that pulmonary artery enlargement may have developed secondary to COPD in our subject group.

We also explored the relationship between pulmonary artery volumes and exacerbations of COPD. In the resultant significant model that explained total COPD exacerbations in 68 ex-smokers with airflow limitation, previous exacerbations were not a significant predictor, which was surprising in light of previous work.[26] However, the number of previous

exacerbations was likely not a predictor of total exacerbations as only a single subject experienced 4 previous exacerbations (between 5 years and 2.5 years prior to study). Consistent with previous work that showed the association between 6MWD and COPD hospitalization[48], we observed that the 6MWD was a significant predictor in our multivariate model and reported that a 1m decrease in 6MWD resulted in a two-fold increase in total exacerbations. While in our study, $FEV_1\%_{pred}$ was associated with a 3-fold increase in total exacerbations, previous studies showed that FEV_1 correlated weakly with clinical symptoms including cardiovascular disease and exacerbation frequency.[49, 50] Total pulmonary artery volume was significantly (p=.03) associated with exacerbations while the PA:A ratio which was associated with acute exacerbations of COPD in the COPDGene (n = 3464) and ECLIPSE (n = 2005) studies[3] was not significant in our model. This suggests that the three-dimensional total pulmonary artery volume measurement may have a stronger association with COPD exacerbations than the PA:A ratio.

It is important to address the limitations that we encountered throughout this work. First, we must acknowledge that subject groups consisted of a relatively small sample size as compared to previous studies using the one-dimensional measurement.[3] Our study was limited to and only included those exacerbations that required hospitalizations. Based on a previous study, about 50% of exacerbations go unreported[5] and such events should be considered in future studies as they may provide additional information when predicting future exacerbations. Several studies have shown the relationship between pulmonary artery size and pulmonary hypertension[23-25, 51-54]. It has also been shown that individuals with pulmonary hypertension have an increased risk of experiencing a COPD exacerbation.[48] While we sought to explore the relationship between pulmonary artery enlargement and COPD, it may be of importance to also include pulmonary artery pressure measurements in future analyses. Unfortunately, right-heart catheterization data was not acquired for this group of patients and therefore pulmonary artery pressures could not be directly measured and included in our analyses.

In summary, we demonstrated that pulmonary artery volume changes may develop in very early or subclinical stages of COPD. We also showed that total pulmonary artery volume predicted COPD exacerbations, in a relatively small number of COPD patients in whom there were very few previous exacerbations.

3.5 Acknowledgements

3.6 Declaration of interests

3.7 References

[1] Raherison C, Girodet P. Epidemiology of COPD. European Respiratory Review 2009;18(114):213-21.

[2] Kirby M, Owrangi A, Svenningsen S, et al. On the role of abnormal DLCO in ex-smokers without airflow limitation: symptoms, exercise capacity and hyperpolarised helium-3 MRI. Thorax 2013;68(8):752-9.

[3] Wells JM, Washko GR, Han MK, et al. Pulmonary arterial enlargement and acute exacerbations of COPD. New England Journal of Medicine 2012;367(10):913-21.

[4] Rabe KF, Hurd S, Anzueto A, et al. Global strategy for the diagnosis, management, and prevention of chronic obstructive pulmonary disease: GOLD executive summary. American journal of respiratory and critical care medicine 2007;176(6):532-55.

[5] Burge S, Wedzicha J. COPD exacerbations: definitions and classifications. European Respiratory Journal 2003;21(41 suppl):46s-53s.

[6] Dransfield MT, Huang F, Nath H, Singh SP, Bailey WC, Washko GR. CT emphysema predicts thoracic aortic calcification in smokers with and without COPD. COPD: Journal of Chronic Obstructive Pulmonary Disease 2010;7(6):404-10.

[7] Chae EJ, Seo JB, Oh Y-M, Lee JS, Jung Y, Do Lee S. Severity of Systemic Calcified Atherosclerosis Is Associated With Airflow Limitation and Emphysema. Journal of computer assisted tomography 2013;37(5):743-9.

[8] McAllister DA, MacNee W, Duprez D, et al. Pulmonary function is associated with distal aortic calcium, not proximal aortic distensibility. MESA lung study. COPD: Journal of Chronic Obstructive Pulmonary Disease 2011;8(2):71-8.

[9] Rasmussen T, Køber L, Pedersen JH, et al. Relationship between chronic obstructive pulmonary disease and subclinical coronary artery disease in long-term smokers. European Heart Journal–Cardiovascular Imaging 2013;14(12):1159-66.

[10] Anthonisen NR, Skeans MA, Wise RA, Manfreda J, Kanner RE, Connett JE. The Effects of a Smoking Cessation Intervention on 14.5-Year MortalityA Randomized Clinical Trial. Annals of internal medicine 2005;142(4):233-9.

[11] Sidney S, Sorel M, Quesenberry CP, DeLuise C, Lanes S, Eisner MD. COPD and incident cardiovascular disease hospitalizations and mortality: Kaiser Permanente Medical Care Program. CHEST Journal 2005;128(4):2068-75.

[12] Iwamoto H, Yokoyama A, Kitahara Y, et al. Airflow limitation in smokers is associated with subclinical atherosclerosis. American journal of respiratory and critical care medicine 2009;179(1):35-40.

[13] Barr RG, Ahmed FS, Carr JJ, et al. Subclinical atherosclerosis, airflow obstruction and emphysema: the MESA Lung Study. European Respiratory Journal 2012;39(4):846-54.

[14] Engström G, Hedblad B, Valind S, Janzon L. Asymptomatic leg and carotid atherosclerosis in smokers is related to degree of ventilatory capacity: longitudinal and cross-sectional results from 'Men born in 1914', Sweden. Atherosclerosis 2001;155(1):237-43.

[15] Lahousse L, van den Bouwhuijsen QJ, Loth DW, et al. Chronic obstructive pulmonary disease and lipid core carotid artery plaques in the elderly: the Rotterdam Study. American journal of respiratory and critical care medicine 2013;187(1):58-64.

[16] van Gestel YR, Flu W-J, van Kuijk J-P, et al. Association of COPD with carotid wall intima-media thickness in vascular surgery patients. Respiratory medicine 2010;104(5):712-6.

[17] Frantz S, Nihlén U, Dencker M, Engström G, Löfdahl CG, Wollmer P. Atherosclerotic plaques in the internal carotid artery and associations with lung function assessed by different methods. Clinical physiology and functional imaging 2012;32(2):120-5.

[18] Barr RG, Mesia-Vela S, Austin JH, et al. Impaired flow-mediated dilation is associated with low pulmonary function and emphysema in ex-smokers: the Emphysema and Cancer Action Project (EMCAP) Study. American journal of respiratory and critical care medicine 2007;176(12):1200-7.

[19] Cinarka H, Kayhan S, Gumus A, et al. Arterial stiffness measured by carotid femoral pulse wave velocity is associated with disease severity in chronic obstructive pulmonary disease. Respiratory care 2013;59(2):274-80.

[20] Sabit R, Bolton CE, Edwards PH, et al. Arterial stiffness and osteoporosis in chronic obstructive pulmonary disease. American journal of respiratory and critical care medicine 2007;175(12):1259-65.

[21] Kim S, Yoon D, Lee E, et al. Carotid atherosclerosis in patients with untreated chronic obstructive pulmonary disease. The International Journal of Tuberculosis and Lung Disease 2011;15(9):1265-70.

[22] Pike D, Kirby M, Lindenmaier TJ, et al. Pulmonary Abnormalities and Carotid Atherosclerosis in Ex-Smokers without Airflow Limitation. COPD: Journal of Chronic Obstructive Pulmonary Disease 2014.

[23] Ackman Haimovici JB, Trotman-Dickenson B, Halpern EF, et al. Relationship between pulmonary artery diameter at computed tomography and pulmonary artery pressures at right-sided heart catheterization. Academic radiology 1997;4(5):327-34.

[24] Kuriyama K, Gamsu G, Stern RG, Cann CE, Herfkens RJ, Brundage BH. CT-determined pulmonary artery diameters in predicting pulmonary hypertension. Investigative radiology 1984;19(1):16-22.

[25] Lange TJ, Dornia C, Stiefel J, et al. Increased pulmonary artery diameter on chest computed tomography can predict borderline pulmonary hypertension. Pulmonary circulation 2013;3(2):363.

[26] Hurst JR, Vestbo J, Anzueto A, et al. Susceptibility to exacerbation in chronic obstructive pulmonary disease. New England Journal of Medicine 2010;363(12):1128-38.

[27] Global Initiative for Chronic Lung Disease. Global strategy for the diagnosis, management, and prevention of chronic obstructive pulmonary disease (Updated 2013). In, 2013

[28] Gudmundsson G, Ulrik CS, Gislason T, et al. Long-term survival in patients hospitalized for chronic obstructive pulmonary disease: a prospective observational study in the Nordic countries. International journal of chronic obstructive pulmonary disease 2012;7:571-6.

[29] Kirby M, Pike D, Coxson HO, McCormack DG, Parraga G. Hyperpolarized 3He ventilation defects used to predict pulmonary exacerbations in mild to moderate chronic obstructive pulmonary disease. Radiology 2014;273(3):887-96.

[30] Miller MR, Hankinson J, Brusasco V, et al. Standardisation of spirometry. Eur Respir J 2005;26(2):319-38.

[31] Jones PW, Quirk FH, Baveystock CM, Littlejohns P. A self-complete measure of health status for chronic airflow limitation: the St. George's Respiratory Questionnaire. American Review of Respiratory Disease 1992;145(6):1321-7.

[32] Jones PW, Quirk F, Baveystock C. The St George's respiratory questionnaire. Respiratory medicine 1991;85:25-31.

[33] Enright PL. The six-minute walk test. Respiratory care 2003;48(8):783-5.

[34] Parraga G, Ouriadov A, Evans A, et al. Hyperpolarized 3He ventilation defects and apparent diffusion coefficients in chronic obstructive pulmonary disease: preliminary results at 3.0 Tesla. Investigative radiology 2007;42(6):384-91.

[35] Kirby M, Svenningsen S, Owrangi A, et al. Hyperpolarized 3He and 129Xe MR imaging in healthy volunteers and patients with chronic obstructive pulmonary disease. Radiology 2012;265(2):600-10.

[36] Vestbo J, Anderson W, Coxson HO, et al. Evaluation of COPD longitudinally to identify predictive surrogate end-points (ECLIPSE). European Respiratory Journal 2008;31(4):869-73.

[37] Shrimpton P, Jones D. Normalised organ doses for x ray computed tomography calculated using Monte Carlo techniques and a mathematical anthropomorphic phantom. Radiation Protection Dosimetry 1993;49(1-3):241-3.

[38] Kirby M, Heydarian M, Svenningsen S, et al. Hyperpolarized ^{3}He Magnetic Resonance Functional Imaging Semiautomated Segmentation. Academic radiology 2012;19(2):141-52.

[39] Woodhouse N, Wild JM, Paley MN, et al. Combined helium-3/proton magnetic resonance imaging measurement of ventilated lung volumes in smokers compared to never-smokers. Journal of magnetic resonance imaging 2005;21(4):365-9.

[40] Kirby M, Heydarian M, Wheatley A, McCormack DG, Parraga G. Evaluating bronchodilator effects in chronic obstructive pulmonary disease using diffusion-weighted hyperpolarized helium-3 magnetic resonance imaging. Journal of Applied Physiology 2012;112(4):651-7.

[41] Nakano Y, Muro S, Sakai H, et al. Computed tomographic measurements of airway dimensions and emphysema in smokers: correlation with lung function. American journal of respiratory and critical care medicine 2000;162(3):1102-8.

[42] Gevenois PA, De Maertelaer V, De Vuyst P, Zanen J, Yernault J-C. Comparison of computed density and macroscopic morphometry in pulmonary emphysema. American journal of respiratory and critical care medicine 1995;152(2):653-7.

[43] Mishima M, Hirai T, Itoh H, et al. Complexity of terminal airspace geometry assessed by lung computed tomography in normal subjects and patients with chronic obstructive pulmonary disease. Proceedings of the National Academy of Sciences 1999;96(16):8829-34.

[44] Ainsworth CD, Blake CC, Tamayo A, Beletsky V, Fenster A, Spence JD. 3D Ultrasound Measurement of Change in Carotid Plaque Volume A Tool for Rapid Evaluation of New Therapies. Stroke; a journal of cerebral circulation 2005;36(9):1904-9.

[45] Lindenmaier TJ, Sheikh K, Bluemke E, et al. Three-dimensional segmentation of pulmonary artery volume from thoracic computed tomography imaging. In. SPIE Proceedings, 2015: 94172O-O-8

[46] Lambert D. Zero-inflated Poisson regression, with an application to defects in manufacturing. Technometrics 1992;34(1):1-14.

[47] Chaouat A, Naeije R, Weitzenblum E. Pulmonary hypertension in COPD. European Respiratory Journal 2008;32(5):1371-85.

[48] Kessler R, Faller M, Fourgaut G, Mennecier B, Weitzenblum E. Predictive factors of hospitalization for acute exacerbation in a series of 64 patients with chronic

obstructive pulmonary disease. American journal of respiratory and critical care medicine 1999;159(1):158-64.

[49] Franciosi LG, Page CP, Celli BR, et al. Markers of disease severity in chronic obstructive pulmonary disease. Pulmonary pharmacology & therapeutics 2006;19(3):189-99.

[50] Gelb AF, Hogg JC, Müller NL, et al. Contribution of emphysema and small airways in COPD. CHEST Journal 1996;109(2):353-9.

[51] Chan AL, Juarez MM, Shelton DK, et al. Novel computed tomographic chest metrics to detect pulmonary hypertension. BMC medical imaging 2011;11(1):7.

[52] Burger IA, Husmann L, Herzog BA, et al. Main pulmonary artery diameter from attenuation correction CT scans in cardiac SPECT accurately predicts pulmonary hypertension. Journal of Nuclear Cardiology 2011;18(4):634-41.

[53] Edwards P, Bull R, Coulden R. CT measurement of main pulmonary artery diameter. The British journal of radiology 1998;71(850):1018-20.

[54] Tan RT, Kuzo R, Goodman LR, Siegel R, Haasler GB, Presberg KW. Utility of CT scan evaluation for predicting pulmonary hypertension in patients with parenchymal lung disease. CHEST Journal 1998;113(5):1250-6.

CHAPTER 4: CONCLUSIONS AND FUTURE WORK

4.1 Summary

COPD exacerbations are severe events that result in decreased health-related quality of life and contribute to increased morbidity and greater mortality rates.[1, 2] Exacerbations are also of major impact on our healthcare system, as hospitalizations associated with treatment of these events are costly.[3-5] It has been previously shown that the frequency of exacerbations increases with the severity of COPD and that this is an independent determinant of health-related patient quality of life.[1, 2] Biomarkers for predicting the occurrence of exacerbations have not been well established; however, numerous studies have outlined several risk factors, such as a decreased exercise capacity, that are associated with a higher exacerbation frequency.[6-8] In particular, Hurst et al. demonstrated that, in a group of 2138 subjects, the single best predictor of future exacerbations was the occurrence of previous exacerbations. This was consistent in COPD patients across GOLD severity grades.[7] A further study by Wells et al., which included 3464 subjects from the COPDGene study as well as 2005 individuals from the ECLIPSE study, showed that a pulmonary artery to aorta diameter ratio >1 was associated with a history of acute exacerbations.[8] Furthermore, this ratio was associated with risk factors of future exacerbations.[8] However, this study was limited in that it relied on a simple one-dimensional diameter measurement. We believe that such a measurement is not sensitive to three-dimensional morphological changes of the pulmonary vasculature, as morphological changes could vary in different dimensions. A three-dimensional volumetric measurement approach would be more sensitive in quantifying changes in pulmonary artery size because it would account for morphological changes in all three Cartesian planes and would take into consideration a larger section of the vessel.

Therefore, the objectives of this thesis were the following: 1) to develop a three-dimensional technique for assessing the size of the main, left and right pulmonary arteries; 2) to determine the inter- and intra-observer reducibility of our approach; 3) to determine associations between pulmonary artery volumes and COPD; and, 4) to evaluate pulmonary artery volumes as useful biomarkers for predicting COPD exacerbations.

In Chapter 2, we address objective 1 which focuses on the development of a three-dimensional volumetric technique and on the assessment of its inter- and intra-observer reproducibility. Briefly, to determine the volume, we manually outlined the cross-sectional area of each artery in a series of slices perpendicular to the longitudinal axis of the vessel. Summing the products of each area and inter-slice distance resulted in a volume measurement for each vessel. Total pulmonary artery volume was also calculated by taking the union of voxels enclosed by each of the three vessels and multiplying it by the voxel dimensions. From five rounds of repeated measurements, performed by three observers, we showed that our technique was highly reproducible, with strong inter- and intra-observer agreement between measurements. To assess the inter- and intra-observer agreement, the coefficient of variation as well as the intraclass correlation coefficient was calculated from the five repeated rounds of measurements. We also showed strong agreement between baseline and follow-up measurements performed by the same observer with four months between measurements.

In Chapter 3, we address objective 2, which focuses on evaluating PA abnormalities in a group of ex-smokers. Specifically, we: 1) compared pulmonary artery sizes between a group of never-smokers and a group of ex-smokers; 2) assessed the relationship between pulmonary artery volumes and measurements of lung function and structure; and, 3) assessed pulmonary artery volumes as potential biomarkers for predicting the occurrence of acute exacerbations. We hypothesized that pulmonary artery volumes will be greater in ex-smokers as compared to never-smokers. We expected pulmonary artery volumes to correlate with measurements of lung function and structure and that they would be a suitable biomarker for predicting exacerbations of COPD. We observed that ex-smokers presented with higher artery volumes than did the never-smoker subject group. When all ex-smokers were grouped together, we found significant positive correlations between VDP and MPA, LPA, RPA and TPA volumes. Furthermore, multivariate regression analysis revealed total pulmonary artery volume to be a significant predictor of COPD exacerbations; however, this relationship should be tested in different subject groups to strengthen our finding.

4.2   Limitations of Current Work

It is important that we report the limitations that were encountered in developing the volumetric technique described in Chapter 2 as well as the clinical relationships described in Chapter 3. Although measurements were reproducible with high inter- and intra-observer agreement, when examining measurements performed by each observer in more detail, we found that most of the variability between measurements resulted from the angle at which the axes of segmentation were placed. Better anatomical landmarks should be considered when placing the axes of segmentation to further improve the reproducibility of our technique. Furthermore, manual segmentation makes this technique time consuming and laborious. Automation of the technique would address this limitation. Moreover, we must acknowledge the fact that the computed tomography images acquired for our subjects were intended for emphysema measurements of the lung. For this reason, in several images it was difficult to distinguish the pulmonary artery from the surrounding tissue. Contrast imaging using an iodine-based contrast agent would allow the pulmonary artery to be better defined from the surroundings and potentially improve the reproducibility of our technique.

When assessing the relationship between pulmonary artery volumes and measurements of lung function and structure, we must acknowledge that our subject groups consisted of a relatively small sample size as compared to previous studies using the one-dimensional measurement.[8] Thus, our technique should be extended to different subject groups to evaluate its association with COPD and its ability to predict exacerbations. Furthermore, 14 subjects were excluded from our analyses due to poor image quality, which often resulted from poor contrast between the pulmonary arteries and the surrounding tissue. Our study was limited to and only included those exacerbations that required hospitalizations. Based on a previous study, about 50% of exacerbations go unreported. These events should be considered and included in future analyses. Several studies have shown the relationship between pulmonary artery size and pulmonary hypertension.[9-15] It has also been shown that individuals with pulmonary hypertension have an increased risk of experiencing a COPD exacerbation.[6] While we sought to explore the relationship between pulmonary artery enlargement and COPD, it may be of importance to also include pulmonary artery pressure measurements in future analyses. Unfortunately, right-heart

catheterization data was not collected for this group of patients and therefore pulmonary artery pressures could not be directly measured and included in our analyses.

4.3 Future work and Clinical Applications

As previously mentioned, when assessing the relationship between pulmonary artery size and COPD, we were limited by a relatively small sample size for both the ex-smoker and the never-smoker subject group. Wells et al. explored the relationship between pulmonary artery diameter and exacerbations in a large number of subjects.[8] Future studies should consider assessing the relationship between pulmonary artery volumes and COPD exacerbations in a large number of subjects as well as in different subject groups, including healthy individuals.

To our knowledge we are the first to consider a three-dimensional technique for assessing the size of the main, left and right pulmonary arteries. As mentioned before, manual slice-by-slice segmentation of the pulmonary arteries in cross-sectional planes to each vessel are time consuming and laborious. The time taken to perform main, left and right pulmonary artery volume measurements for a single subject can take up to one hour. The extensive amount of time required to analyze a single individual makes our technique unsuitable for large scale clinical trials. Therefore, future work should focus on improving our technique by developing semi-automated or fully-automated algorithms to estimate the size of the pulmonary arteries. Automation of this technique will reduce the user input required and would therefore significantly decrease the time taken to perform a measurement. Such an improvement would allow pulmonary artery volumes to be measured in studies with larger sample sizes. The use of iodine-based contrast agents may be considered in future studies to improve the contrast between the pulmonary arteries and the surrounding tissues. This, in turn, may help with developing an appropriate automated algorithm which estimates the size of the pulmonary artery on a specific threshold and boundaries set by the user.

Pulmonary hypertension is a known complication of COPD that results in an increase in morbidity and mortality.[16] The current gold standard for assessing pulmonary hypertension is through right heart catheterization.[9] This technique is invasive, generally causes

discomfort, and can lead to complications. Recent studies have shown that the diameter of the pulmonary artery measured at the level of the bifurcation has the ability to predict borderline pulmonary hypertension.[9-15] We believe that our three-dimensional volumetric technique may be more sensitive to morphological changes in the pulmonary artery and should therefore be assessed as a potential diagnostic tool in predicting pulmonary hypertension. This would provide a non-invasive method for assessing and monitoring patients at risk of pulmonary hypertension. Therefore, future studies should assess the relationship between pulmonary artery pressures measured by right heart catheterization and pulmonary artery volumes measured using our technique.

Future studies should also focus on developing MRI imaging techniques for evaluating the size of the pulmonary arteries. This development would allow for repeated measurements to be performed and would therefore permit evaluation of disease progression and treatment response. MRI provides high soft tissue contrast which may yield useful information in developing future measurements of the pulmonary arteries. Being able to differentiate between the lumen of the vessel and the arterial wall could reveal useful information about pulmonary artery abnormalities.

4.4   References

[1] Seemungal TA, Donaldson GC, Paul EA, Bestall JC, Jeffries DJ, Wedzicha JA. Effect of exacerbation on quality of life in patients with chronic obstructive pulmonary disease. American journal of respiratory and critical care medicine 1998;157(5):1418-22.

[2] Reilly JJ. Stepping down therapy in COPD. New England Journal of Medicine 2014;371(14):1340-1.

[3] Mittmann N, Kuramoto L, Seung S, Haddon J, Bradley-Kennedy C, Fitzgerald J. The cost of moderate and severe COPD exacerbations to the Canadian healthcare system. Respiratory medicine 2008;102(3):413-21.

[4] Connors Jr AF, Dawson NV, Thomas C, et al. Outcomes following acute exacerbation of severe chronic obstructive lung disease. The SUPPORT investigators (Study to Understand Prognoses and Preferences for Outcomes and Risks of Treatments). American journal of respiratory and critical care medicine 1996;154(4):959-67.

[5] Chapman K, Mannino DM, Soriano J, et al. Epidemiology and costs of chronic obstructive pulmonary disease. European Respiratory Journal 2006;27(1):188-207.

[6] Kessler R, Faller M, Fourgaut G, Mennecier B, Weitzenblum E. Predictive factors of hospitalization for acute exacerbation in a series of 64 patients with chronic obstructive pulmonary disease. American journal of respiratory and critical care medicine 1999;159(1):158-64.

[7] Hurst JR, Vestbo J, Anzueto A, et al. Susceptibility to exacerbation in chronic obstructive pulmonary disease. New England Journal of Medicine 2010;363(12):1128-38.

[8] Wells JM, Washko GR, Han MK, et al. Pulmonary arterial enlargement and acute exacerbations of COPD. New England Journal of Medicine 2012;367(10):913-21.

[9] Lange TJ, Dornia C, Stiefel J, et al. Increased pulmonary artery diameter on chest computed tomography can predict borderline pulmonary hypertension. Pulmonary circulation 2013;3(2):363.

[10] Kuriyama K, Gamsu G, Stern RG, Cann CE, Herfkens RJ, Brundage BH. CT-determined pulmonary artery diameters in predicting pulmonary hypertension. Investigative radiology 1984;19(1):16-22.

[11] Chan AL, Juarez MM, Shelton DK, et al. Novel computed tomographic chest metrics to detect pulmonary hypertension. BMC medical imaging 2011;11(1):7.

[12] Burger IA, Husmann L, Herzog BA, et al. Main pulmonary artery diameter from attenuation correction CT scans in cardiac SPECT accurately predicts pulmonary hypertension. Journal of Nuclear Cardiology 2011;18(4):634-41.

[13] Edwards P, Bull R, Coulden R. CT measurement of main pulmonary artery diameter. The British journal of radiology 1998;71(850):1018-20.

[14] Tan RT, Kuzo R, Goodman LR, Siegel R, Haasler GB, Presberg KW. Utility of CT scan evaluation for predicting pulmonary hypertension in patients with parenchymal lung disease. CHEST Journal 1998;113(5):1250-6.

[15] Ackman Haimovici JB, Trotman-Dickenson B, Halpern EF, et al. Relationship between pulmonary artery diameter at computed tomography and pulmonary artery pressures at right-sided heart catheterization. Academic radiology 1997;4(5):327-34.

[16] Chaouat A, Naeije R, Weitzenblum E. Pulmonary hypertension in COPD. European Respiratory Journal 2008;32(5):1371-85.

Appendix A: RESEARCH ETHICS BOARD APPROVAL NOTICES

Western Research

Research Ethics

Western University Health Science Research Ethics Board
HSREB Amendment Approval Notice

Principal Investigator:
Department & Institution: Schulich School of Medicine and Dentistry\Imaging,Robarts Research Institute

HSREB File Number: 6014
Study Title: Longitudinal Study of Helium-3 Magnetic Resonance Imaging of COPD (REB #15930)
Sponsor: UWO Internal Research Fund

HSREB Amendment Approval Date: July 30, 2014
HSREB Expiry Date: March 31, 2018

Documents Approved and/or Received for Information:

Document Name	Comments	Version Date
Revised Western University Protocol		2014/07/07
Revised Letter of Information & Consent	version 12	2014/07/07

The Western University Health Science Research Ethics Board (HSREB) has reviewed and approved the amendment to the above named study, as of the HSREB Initial Approval Date noted above.

HSREB approval for this study remains valid until the HSREB Expiry Date noted above, conditional to timely submission and acceptance of HSREB Continuing Ethics Review. If an Updated Approval Notice is required prior to the HSREB Expiry Date, the Principal Investigator is responsible for completing and submitting an HSREB Updated Approval Form in a timely fashion.

The Western University HSREB operates in compliance with the Tri-Council Policy Statement Ethical Conduct for Research Involving Humans (TCPS2), the International Conference on Harmonization of Technical Requirements for Registration of Pharmaceuticals for Human Use Guideline for Good Clinical Practice Practices (ICH E6 R1), the Ontario Personal Health Information Protection Act (PHIPA, 2004), Part 4 of the Natural Health Product Regulations, Health Canada Medical Device Regulations and Part C, Division 5, of the Food and Drug Regulations of Health Canada.

Members of the HSREB who are named as Investigators in research studies do not participate in discussions related to, nor vote on such studies when they are presented to the REB.

The HSREB is registered with the U.S. Department of Health & Human Services under the IRB registration number

Ethics Officer, on behalf of

Ethics Officer to Contact for Further Information

This is an official document. Please retain the original in your files.

Western Research

Western University Health Science Research Ethics Board
HSREB Amendment Approval Notice

Principal Investigator:
Department & Institution: Schulich School of Medicine and Dentistry\Imaging,Robarts Research Institute

HSREB File Number: 7320
Study Title: Longitudinal 3He Magnetic Resonance Imaging of Healthy Lung (REB #17396)
Sponsor: Canadian Institutes of Health Research

HSREB Amendment Approval Date: June 24, 2014
HSREB Expiry Date: September 30, 2016

Documents Approved and/or Received for Information:

Document Name	Comments	Version Date
Revised Western University Protocol		2014/05/15
Revised Letter of Information & Consent	version 6	2014/05/15

The Western University Health Science Research Ethics Board (HSREB) has reviewed and approved the amendment to the above named study, as of the HSREB Initial Approval Date noted above.

HSREB approval for this study remains valid until the HSREB Expiry Date noted above, conditional to timely submission and acceptance of HSREB Continuing Ethics Review. If an Updated Approval Notice is required prior to the HSREB Expiry Date, the Principal Investigator is responsible for completing and submitting an HSREB Updated Approval Form in a timely fashion.

The Western University HSREB operates in compliance with the Tri-Council Policy Statement Ethical Conduct for Research Involving Humans (TCPS2), the International Conference on Harmonization of Technical Requirements for Registration of Pharmaceuticals for Human Use Guideline for Good Clinical Practice Practices (ICH E6 R1), the Ontario Personal Health Information Protection Act (PHIPA, 2004), Part 4 of the Natural Health Product Regulations, Health Canada Medical Device Regulations and Part C, Division 5, of the Food and Drug Regulations of Health Canada.

Members of the HSREB who are named as Investigators in research studies do not participate in discussions related to, nor vote on such studies when they are presented to the REB.

The HSREB is registered with the U.S. Department of Health & Human Services under the IRB registration number

Ethics Officer to Contact for Further Information

This is an official document. Please retain the original in your files.

Appendix B: PERMISSIONS FOR REPRODUCTION OF SCIENTIFIC ARTICLE

SPIE   TRANSFER OF COPYRIGHT TO SOCIETY OF PHOTO-OPTICAL INSTRUMENTATION ENGINEERS (SPIE)

Title of Paper: Three-Dimensional Segmentation of Pulmonary Artery Volume from Thoracic Computed Tomography Imaging

SPIE Paper Number: (xxxx-xx) 9417-99 **Contact Author Email:** _____

Author(s): _____

This signed statement must be returned to SPIE prior to the scheduled publication of the Proceedings or Journal in which the Paper will be published. The intent of this Agreement is to protect the interests of both SPIE and authors/employers and to specify reasonable rights for both parties related to publication and reuse of the material.

The undersigned hereby assign(s) to Society of Photo-Optical Instrumentation Engineers (SPIE) copyright ownership in the above Paper, effective if and when the Paper is accepted for publication by SPIE and to the extent transferable under applicable national law. This assignment gives SPIE the right to register copyright to the Paper in its name as claimant and to publish the Paper in any print or electronic medium.

Authors, or their employers in the case of works made for hire, retain the following rights:

1. All proprietary rights other than copyright, including patent rights.

2. The right to make and distribute copies of the Paper for internal purposes.

3. The right to use the material for lecture or classroom purposes.

4. The right to prepare derivative publications based on the Paper, including books or book chapters, journal papers, and magazine articles, provided that publication of a derivative work occurs subsequent to the official date of publication by SPIE.

5. The right to post an author-prepared version or an official version (preferred version) of the published paper on an internal or external server controlled exclusively by the author/employer, provided that (a) such posting is noncommercial in nature and the paper is made available to users without charge; (b) a copyright notice and full citation appear with the paper, and (c) a link to SPIE's official online version of the abstract is provided using the DOI (Document Object Identifier) link.

   Citation format:
   Author(s), "Paper Title," Publication Title, Editors, Volume (Issue) Number, Article (or Page) Number, (Year).

   Copyright notice format:
   Copyright XXXX (year) Society of Photo-Optical Instrumentation Engineers. One print or electronic copy may be made for personal use only. Systematic reproduction and distribution, duplication of any material in this paper for a fee or for commercial purposes, or modification of the content of the paper are prohibited.

   DOI abstract link format:
   http://dx.doi.org/DOI# *(Note: The DOI can be found on the title page or online abstract page of any SPIE article.)*

If the work that forms the basis of this Paper was done under a contract with a governmental agency or other entity that retains certain rights, this Transfer of Copyright is subject to any rights that such governmental agency or other entity may have acquired.

By signing this Agreement, the authors warrant that (1) the Paper is original and has not previously been published elsewhere; (2) this work does not infringe on any copyright or other rights in any other work; (3) all necessary reproduction permissions, licenses, and clearances have been obtained; and (4) the authors own the copyright in the Paper, are authorized to transfer it, and have full power to enter into this Agreement with SPIE.

WHO SHOULD SIGN. This form must be signed by (1) at least one author who is not a U.S. Government employee and (2) the author's employer if the Paper was prepared within the scope of the author's employment or was commissioned by the employer. If not signed by all authors, the author(s) signing this Agreement represents that he/she is signing this Agreement as authorized agent for and on behalf of all the authors.

		01/13/2015
Author's signature	Print name	Date (mm/dd/yyyy)
		01/13/2015
Author's signature	Print name	Date (mm/dd/yyyy)
Authorized Employer signature	Print name Title	Date (mm/dd/yyyy)

U.S. GOVERNMENT EMPLOYMENT CERTIFICATION
A work prepared by a U.S. Government employee as part of his or her official duties is not eligible for U.S. Copyright. If all authors were U.S. Government employees when this Paper was prepared, and the authors prepared this Paper as part of their official duties, at least one author should sign below. If at least one author was not a U.S. Government employee, the work is eligible for copyright and that author should sign the Transfer of Copyright form above.

Author's signature	Print name	Date (mm/dd/yyyy)

Curriculum Vitae

Education

2013-Present   **Master's Thesis Candidate - Master of Science - Medical Biophysics**
The University of Western Ontario, London, Ontario, Canada
Thesis: Three-dimensional computed tomography measurements of
      pulmonary artery volumes
Supervisor: Dr. Grace Parraga

2009-2013   **Bachelor of Science**
Medical Biophysics Honors Specialization Program
The University of Western Ontario, London, Ontario, Canada

Undergraduate Thesis at Robarts Research Institute, London, Ontario.
One, Two and Three-Dimensional Ultrasound Measurements of Carotid Atherosclerosis Before and After Cardiac Rehabilitation: Preliminary results of a Randomized Controlled Trial
Supervisor: Dr. Grace Parraga

Publications

[1] **TJ Lindenmaier**, M Kirby, M Mura, C Licskai, HO Coxson, IA Cunningham and G Parraga, *Pulmonary Artery Abnormalities in Ex-smokers with and without Airflow Limitation.* Journal of Chronic Obstructive Pulmonary Disease, To be submitted March 2015.

[2] **TJ Lindenmaier**, K Sheikh, E Bluemke, I Gyacskov, M Mura, C Licskai, L Mielniczuk, A Fenster, IA Cunningham and G Parraga, *Three-Dimensional Segmentation of Pulmonary Artery Volume from Thoracic Computed Tomography Imaging,* SPIE Medical Imaging, Renaissance Orlando, SeaWorld Orlando, Florida, United States, Conference Proceeding, 2015.

[3] D Pike, M Kirby, **TJ Lindenmaier**, K Sheikh , C Neron, DG Hackam, JD Spence, A Fenster, NAM Paterson, HO Coxson, DG McCormack, DD Sin and G Parraga, *Pulmonary Abnormalities and Carotid Atherosclerosis in Ex-Smokers without Airflow Limitation.* Journal of Chronic Obstructive Pulmonary Disease 2015; 12(1):62-70.

[4] D Pike, **TJ Lindenmaier**, D Sin and G Parraga, *Imaging Evidence of the Relationship between Atherosclerosis and Chronic Obstructive Pulmonary Disease*, Imaging in Medicine 2014; 6(1):53-73.

[5] **TJ Lindenmaier**, DN Buchanan, D Pike, T Hartley, RD Reid, JD Spence, R Chan, M Sharma, PL. Prior, N Suskin and G Parraga, *One, Two and Three-Dimensional Ultrasound Measurements of Carotid Atherosclerosis Before and After Cardiac Rehabilitation: Preliminary results of a Randomized Controlled Trial.* Cardiovascular Ultrasound 2013; 11(1):39.

[6] D Buchanan, **T Lindenmaier**, S Mckay, Y Bureau, DG Hackam, A Fenster, and G Parraga, *The Relationship Of Carotid Three-Dimensional Ultrasound Vessel Wall Volume With Age and Sex: Comparison to Carotid Intima-Media Thickness.* Ultrasound in Med. & Biol. 2012; 38(7):1145–1153.

[7] D Buchanan, I Gyacskov, E Ukwatta, **T Lindenmaier**, A Fenster and G Parraga, *Semi-automated segmentation of carotid artery plaque volume from three-dimensional ultrasound carotid imaging.* SPIE Medical Imaging, Town & Country Resort and Convention Center San Diego, California, USA, February 4-9, Presentation Proceeding 2012.

Conference Presentations and Posters

[1] **TJ Lindemaier**, M Kirby, HO Coxson, M Mura, C Licskai, IA Cunningham, L Mielniczuk and G Parraga, *Left Pulmonary Artery Volume Predicts Acute Exacerbations in COPD: Results of the TINCAN Cohort Study*, American Thoracic Society (ATS), Denver, Colorado, USA, May 15-20 2015, Poster presentation.

[2] **TJ Lindenmaier**, K Sheikh, E Bluemke, I Gyacskov, M Mura, C Licskai, L Mielniczuk, A Fenster, IA Cunningham and G Parraga, *Three-Dimensional Segmentation of Pulmonary Artery Volume from Thoracic Computed Tomography Imaging.* SPIE Medical Imaging, Renaissance Orlando at SeaWorld, Orlando, Florida, United States, February 21-26, 2015, Poster Presentation.

[3] **TJ Lindenmaier**, D Pike, LM Mielnicsuk, C Licskai, M Mura, IA Cunningham and G Parraga, *Pulmonary artery abnormalities in ex-smokers with and without airflow limitation: Relationship to emphysema and airways disease.* Robarts Research Institute Retreat, London, Ontario, Canada, June 9 2014, Poster Presentation.

[4] **TJ Lindenmaier**, D Pike, LM Mielniczuk, JA White, DG McCormack and G Parraga, *An Airways Disease Dominant Phenotype of Pulmonary Artery Enlargement in Chronic Obstructive Pulmonary Disease.* American Thoracic Society (ATS), Town & Country Resort and Convention Center San Diego, California, USA, May 16-21, 2014, Poster Presentation.

[5] **T Lindenmaier**, D Pike, L Mielnicsuk, C Licskai, M Mura, I Cunningham and G Parraga, *Pulmonary artery abnormalities in ex-smokers with and without airflow limitation: Relationship to emphysema and airways disease.* 12th Annual Imaging Network Ontario (ImNO) Symposium, Toronto, Ontario, Canada, March 24-25, 2014, Poster Presentation.

[6] **T Lindenmaier**, D Pike, L Mielnicsuk, C Licskai, M Mura, I Cunningham and G Parraga, *Pulmonary artery abnormalities in ex-smokers with and without airflow limitation: Relationship to emphysema and airways disease.* 4th Annual London Health Research Day, London, Ontario, Canada, March 18, 2014, Poster Presentation.

[7] D Buchanan, **T Lindenmaier**, I Gyacskov, E Ukwatta, A Fenster and G Parraga, *Semi-automated Segmentation of Three Dimensional Ultrasound Carotid Atherosclerotic Plaque Volume*. 3rd North American Summer School on Image Guided Interventions,

Surgical Robotics & Simulation. London, Ontario, August 13-17, 2012, Poster Presentation.

[8] D Buchanan, I Gyacskov, E Ukwatta, **T Lindenmaier**, A Fenster and G Parraga, *Semi-automated segmentation of carotid artery plaque volume from three dimensional ultrasound carotid imaging.* SPIE Medical Imaging, Town & Country Resort and Convention Center San Diego, California, USA, February 4-9, 2012, Podium Presentation.

Scholarships and Awards

2013-2015   The CIHR Strategic Training Program in Vascular Research
CIHR Strategic Training Initiatives in Health Research, $24000

2013-2015   Western Graduate Research Scholarship
The University of Western Ontario, $1500/term = $7500

2010, 2012   Dean's Honor List
Awarded to a full time student who has maintained an average of 80% or more – The University of Western Ontario

2009   Queen Elizabeth II Aiming for the Top Scholarship
Ontario Government Award of Merit, $3500

2009   The Western Scholarship of Distinction
The University of Western Ontario, $1500

2009   Ontario Scholar
Awarded to high school graduates in Ontario with an average of 80% or more in their six best grade 12 courses

Volunteer and work experience

2014-*Present*   Mentor/Tutor at Tutor Doctor, London, Ontario
Responsibilities included: In home tutoring of mathematics and sciences for high school students

2012-2013   Undergraduate Thesis at Robarts Research Institute, London, Ontario.
3D Ultrasound Reconstruction: Monitoring the Progression of Atherosclerosis in Transient Ischemic Stroke Victims
Supervisor: Dr. Grace Parraga

2012   Summer Student at Robarts Research Institute, London, Ontario
Three Dimensional Ultrasound Measurements of the Human Carotid Artery, Supervisor: Dr. Grace Parraga

2011-2012 Student Assistant at Robarts Research Institute, London Ontario
Three Dimensional Ultrasound Measurements of the Human Carotid Artery, Supervisor: Dr. Grace Parraga

2011 Summer Student at Robarts Research Institute, London, Ontario
Three Dimensional Ultrasound Measurements of the Human Carotid Artery, Supervisor: Dr. Grace Parraga

2010 Off to Western Hometown Volunteer, Toronto, Ontario
University of Western Ontario

2006-2009 Sales associate at Zellers Shoppers World, Toronto, Ontario
Responsibilities included: ensuring prompt customer care and satisfaction, organizing and keeping inventory of the merchandise, and working with the cash register and handling money. Customer satisfaction was a main concern.

Languages
English, Hungarian, Romanian